Journal of South American Earth Sciences 50 (2014) 48–66

Contents lists available at ScienceDirect

Journal of South American Earth Sciences

journal homepage: www.elsevier.com/locate/jsames

Emplacement of the La Peña alkaline igneous complex, Mendoza, Argentina (33° S): Implications for the early Miocene tectonic regime in the retroarc of the Andes

D.S. Pagano [a,*], M.A. Galliski [a], M.F. Márquez-Zavalía [a,b]

[a] Departamento de Mineralogía, Petrografía y Geoquímica, IANIGLA, CCT-Mendoza, CONICET, Av. Ruiz Leal s/n, Parque Gral. San Martín, 5500 Mendoza, Argentina
[b] Mineralogía y Petrología, FAD, Universidad Nacional de Cuyo, Centro Universitario, 5502 Mendoza, Argentina

ARTICLE INFO

Article history:
Received 28 August 2013
Accepted 24 December 2013

Keywords:
Alkaline complex
Miocene
Shear zone
Transtensive regime
Precordillera
Mendoza

ABSTRACT

The La Peña alkaline complex (LPC) of Miocene age (18–19 Ma) lies on the eastern front of the Precordillera (32°41′34″S, 68°59′48″W, 1400–2900 m a.s.l.), 30 km northwest of Mendoza city, Argentina. It is a subcircular massif of 19 km^2 and 5 km in diameter, intruded in the metasedimentary sequence of the Villavicencio Formation of Silurian-Devonian age. It is the result of integration of multiple pulses derived from one or more deep magma chambers, which form a suite of silicate rocks grouped into: a clinopyroxenite body, a central syenite facies with a large breccia zone at the contact with the clinopyroxenite, bodies of malignite, trachyte and syenite porphyry necks, and a system of radial and annular dikes of different compositions. Its subcircular geometry and dike system distribution are frequent features of intraplate plutons or plutons emplaced in post-orogenic settings. These morphostructural features characterize numerous alkaline complexes worldwide and denote the importance of magmatic pressures that cause doming with radial and annular fracturing, in a brittle country rock. However, in the LPC, the attitude of the internal fabric of plutonic and subvolcanic units and the preferential layout of dikes match the NW–SE extensional fractures widely distributed in the host rock. This feature indicates a strong tectonic control linked to the structure that facilitate space for emplacement, corresponding to the brittle shear zone parallel to the N–S stratigraphy of the country rock. Shearing produced a system of discontinuities, with a *K* fractal fracture pattern, given by the combination of Riedel (R), anti-Riedel (R′), (P) and extensional (T) fracture systems, responsible for the control of melt migration by the opening of various fracture branches, but particularly through the NW–SE (T) fractures. Five different pulses would have ascent, (1) an initial one from which cumulate clinopyroxenite was formed, (2) a phase of mafic composition represented by dikes cross-cutting the clinopyroxenite, (3) a malignite facies that causes a small breccia in the clinopyroxenite, (4) a central syenite facies that develops breccias at the contact with the clinopyroxenite and, finally, (5) porphyry necks and a system of radial dikes intruding all units. At the moment of the emplacement different mechanisms would have acted, they summarized in: 1) opening of discontinuities synchronous to the magma circulation as the principal mechanism for formation of dikes and conduits; 2) stoping processes, that play an important role in the development of the breccia zone and enabling an efficient transference of material during the emplacement of the syenitic magma and 3) shear-related deformation (regional stress), affected the internal fabric of the facies, causing intracrystalline deformation and submagmatic flow, which is very evident in the central syenite intrusive. The kinematic analysis of shear planes allows proposing that emplacement of the LPC took place in a transtensive regime, which would have occurred in the back-arc of the Andes orogen, during a long period spanning from Miocene to the present, of the compressive deformation responsible, westward and at the same latitude, for the development of the Aconcagua fold and thrust belt.

1. Introduction

Shapes and dimensions of intrusive igneous bodies are frequently the result of interaction and competition between magmatic

Abbreviations: LPC, La Peña Complex; Cc, cumulate clinopyroxenite; Emd, early mafic dikes; Lmd, late mafic dikes; IU, internal unit; EU, external unit.

* Corresponding author. Tel.: +54 261 524 4238.
E-mail addresses: dpagano@mendoza-conicet.gob.ar, dpagano@hotmail.com.ar (D.S. Pagano), galliski@mendoza-conicet.gob.ar (M.A. Galliski), mzavalia@mendoza-conicet.gob.ar (M.F. Márquez-Zavalía).

0895-9811/$ – see front matter © 2013 Elsevier Ltd. All rights reserved.
http://dx.doi.org/10.1016/j.jsames.2013.12.009

pressures and regional stress field. The former arise from internal magma chamber dynamics and their magnitude is directly proportional to the viscosity of the magma. Local or regional stresses, instead, depend on the regional tectonic stress field and crustal/lithospheric vertical density variations, and affect both the country rock and the intrusive body. When tectonic stress is dominant, igneous bodies adjust to regional structures. Conversely, if magmatic pressures dominate, as occurs in intraplate or post-orogenic environments, the bodies take dome shapes and display circular or slightly elliptic sections, with common development of radial and annular fractures hosting dikes of different compositions. These last structures are frequent in alkaline complexes, such as observed in numerous examples around the world (e.g.: Araxá, Traversa et al., 2001; Tapira, Brod et al., 2005; Catalao I, Ribeiro et al., 2005; and Salitre II, Barbosa et al., 2012 in Brazil, or Khibina, Lovozero and Kovdor, Arzamastsev et al., 2000, in Russia). In this paper we study the LPC which represent an opportunity for studying interaction and competition between magmatism and regional stress. We perform a classical structural analysis, based on the study of magmatic structures and contemporary host rock structures. We use concepts related to magmatic structures and their application to the emplacement of widely researched plutons (e.g.: Holder, 1979; Hutton, 1982, 1988; Guillet et al., 1985; Gapais and Barbarin, 1986; Paterson et al., 1989, 1998; Hutton et al., 1990; Clemens and Mawer, 1992; Hutton and Reavy, 1992; Paterson and Vernon, 1995; Petford, 1996; de Saint Blanquat and Tikoff, 1997; Dehls et al., 1998; Vernon, 2000; Pinotti et al. 2002, 2010; Vernon et al., 2004; Žák et al., 2006; D'Eramo et al., 2006, 2010; Pignotta and Paterson, 2007; Vegas et al., 2007) to adapt them to the study of a system compositionally different from the granitic systems to which they are normally applied. The internal structure of the LPC is described at the meso and microscopic scales, with emphasis on its magmatic fabric, to elucidate the genesis and dynamics that favored its emplacement. Finally, we develop a model that fits those structural patterns to estimate their morphology and deep internal structure and we propose a tectonic regimen linked to emplacement, with implications in the Early Miocene tectonic regime in the retroarc of the Andes.

2. Methodology

The LPC mapping was based on ASTER GDEM images, as well as on Google Earth images obtained by Stitch Maps software, supplemented with published references for the area. With the basic information obtained, all transects needed for the geological and structural survey, as well as the sampling sites of the different units, were defined. Finally, a detailed structural survey of discontinuities (faults and joints) was performed on the field. Different sampling areas were selected according to the internal structure of the magmatic facies, sampling for microstructural and petrographic analyses of core and border facies and special magmatic structures. Country rock structures were also mapped on images and in the field, mainly faults and joint fissures. The study of thin sections was performed using a polarizing microscope, and the classification of the igneous rocks was based on modal counting and the IUGS system (Le Maitre, 2002).

To develop the intrusion model magmatic foliations, position of dikes and attitude and kinematics of structures in host rock were considered. The morphology of the body at depth was estimated from the characteristics of the contacts, its internal fabric, and from comparative analysis with the deep internal structure of other alkaline complexes known from gravimetric surveys.

3. Geological setting

At the studied latitude, southeastern of the Andes Centrales, the Argentine Andes include three different morphostructural units of strike N–S, referred as Principal Cordillera, Frontal Cordillera and Precordillera, the latter form an N–S trending mountain chain of 450 km long and 80 km wide. North of 32°30′S, traditional models for the Precordillera fold and thrust belt have involved a thin-skinned tectonic style with complete detachment of a deformed sedimentary cover from a basement dipping gently to the west (Ramos et al., 1986; Allmendinger et al., 1990; von Gosen, 1992). However, in the southern sector, the belt has particular characteristics that reflect a thickskinned tectonic style (von Gosen, 1995; Folguera et al., 2001; Vergés et al., 2007). The Puesto La Peña igneous complex (Villar and Zappettini, 2000) or La Peña (Lucassen et al., 2007), from now on referred as La Peña Complex (LPC), is situated on the eastern border of the Precordillera, 30 km northwest of Mendoza city, between 1400 and 2900 m above sea level (Fig. 1A). This complex is emplaced in a clastic metasedimentary sequence called Villavicencio Formation (Harrington, 1941), made up of N–S striking beds of mudstone, sandstone and conglomerates with turbidity arrangements (González Bonorino, 1975a, b). These deposits, which are ascribed to a Silurian-Devonian age (Cuerda et al., 1993), were affected by the Chanic diastrophic phase of the Late to Middle Devonian, dated at 385 Ma (Davis et al., 2000). This tectonic phase tectonized and metamorphosized the Silurian-Devonian beds generating varying degrees and styles of deformation with increased intensity westward (Giambiagi et al., 2011).

The LPC is a small intrusive complex of roughly circular section, slightly elongated northeast-southwest, 19 km^2 in area and 5 km in diameter, emplaced in the eastern part of the Villavicencio Formation (Fig. 1B). It has straight and high-angle contacts with the country rock, concordant with the stratigraphy in the eastern border and discordant to it in the rest of the complex. It is a plutonic, potassium subsaturated complex, of a malignite–borolanite nature (Villar and Zappettini, 2000) made up mostly of clinopyroxenites, syenites with malignite facies and a system of dikes of diverse compositions (trachyte and mafic dikes). Its Miocene age (Zappettini et al., 2005; Lucassen et al., 2007) places it within the framework of the Andean orogeny, as an atypical expression of the magmatism of the Central Andes.

The LPC was detected during explorations for porphyry copper deposits undertaken in the 1960's by the Dirección General de Fabricaciones Militares. A report by Mezzetti (1968) describes the geology, petrography and ore-petrography, the geochemistry and geophysics and the result of three exploratory drills. Méndez et al. (1995), in a regional study of metallogenesis, contributed with two K–Ar ages performed on whole rock, which yielded quite different results: 43 ± 2 Ma and 27 ± 1 Ma. Later on, Villar and Zappettini (2000) described the geology, petrography and geochemistry of LPC. Villar et al. (2002) published the mineralogy and the chemical composition of the main facies. Zappettini et al. (2005) dated the malignite facies, which yielded an age of 18.7 ± 0.5 Ma. Lucassen et al. (2007) released data on isotope geochemistry of these rocks. They contributed new datings which yielded ages 18.8 ± 0.5, 17.9 ± 0.5, 18.5 ± 0.5 and 19.5 ± 0.6 Ma. The last contributions to the complex geology and mineralogy were made by Zappettini et al. (2008, 2009 and 2013).

3.1. Tectonic setting

The long history of deformation of the western Gondwana margin has gone through several episodes of contractional, extensional and strike-slip deformation (Ramos, 1988; Mpodozis and Ramos, 1989), which are recorded in the Precordillera and Frontal Cordillera, where at least four deformation events are recognized as having occurred during the Early Paleozoic (Ocloyic and Chanic Orogenies), Early Permian (contractional stage of the San Rafael orogeny), Late Permian-Middle Triassic (extensional stage) and

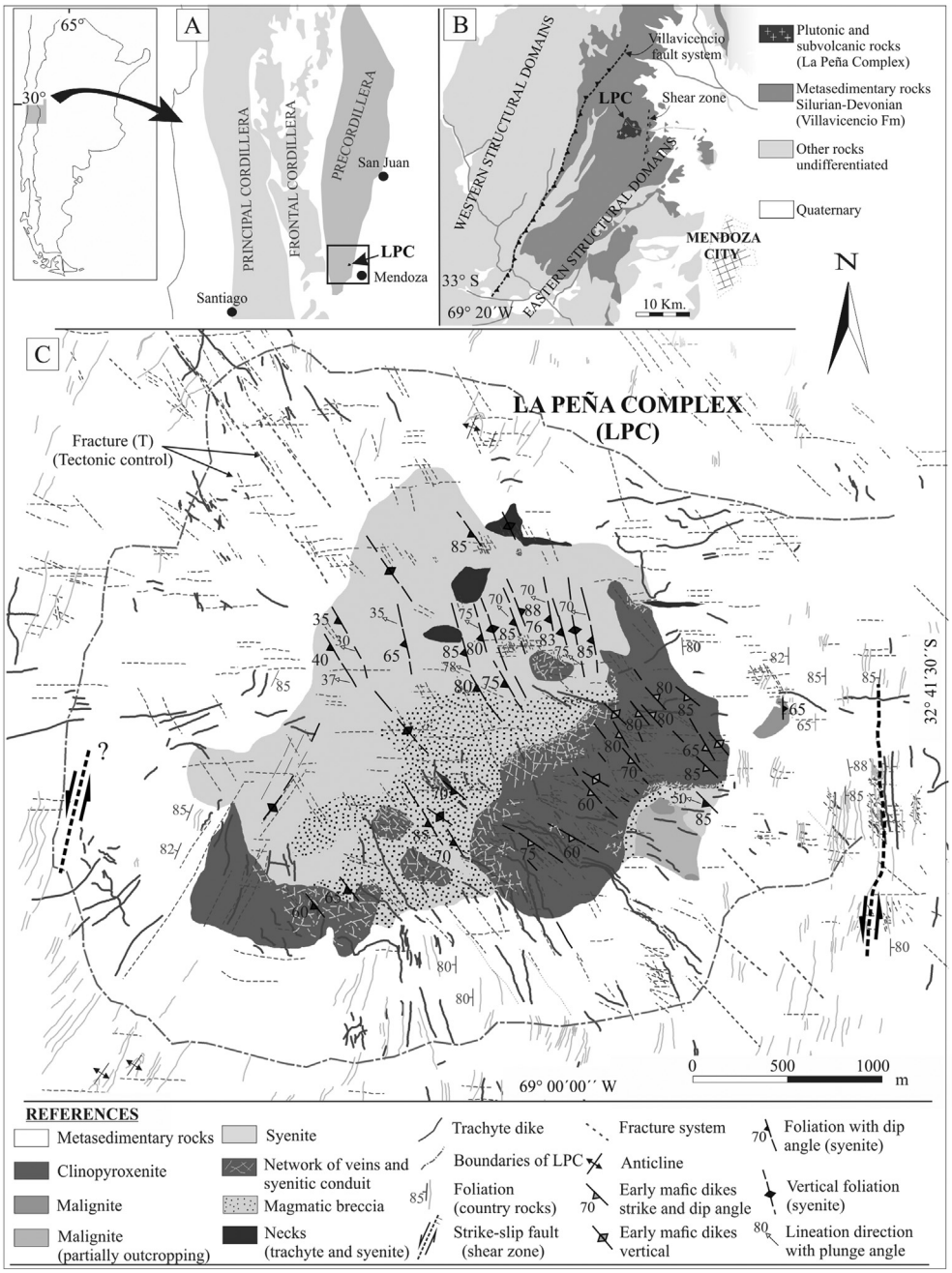

Fig. 1. Location of the study area and geological and structural map. A) Schematic location of the study area in the Precordillera. B) Simplified geological map of the southern part of the Precordillera, representing the Villavicencio Formation and the LPC, with indication of the shear zone located east of the intrusive and the Villavicencio fault system dividing the Precordillera into two structural domains; modified from Giambiagi et al. (2011). C) Geological and structural map of the LPC; showing the lithological units composing the complex and the host rock and its internal structure with traces of foliation and lineation in syenite, strike of ultramafic dikes in clinopyroxenite. Country rock structures are shown: foliation, folds, fracture systems and shear zone. Note the northwest-southeast fractures, highlighted with dashed grey line.

Miocene-Holocene (compressive stage of Andean cycle). The Precordillera, at the latitudes of the study area, responds to a bivergent fault system that can be divided into western and eastern structural domains, split by a disruption zone known as Villavicencio fault system (Fig. 1B), which is considered the main tectonic boundary between both domains (Giambiagi et al., 2011). According to these authors, the western domain is characterized by a complex structural framework, with WNW trending faults, mostly west-vergent, and with complex cross-cutting relationships between predominant strike-slip faults and less frequent dip-slip faults. The eastern domain, however, would have been deformed by homogeneous pure shear and is primarily characterized by reverse dip-slip faults with north-south and NNE strike and predominantly east-vergent. Both domains record the complex and long history of deformation of the Gondwana's Pacific margin, from the early Paleozoic to the Cenozoic. The Villavicencio Formation mostly outcrops in the eastern structural domain and is bounded on the west by the Villavicencio fault system, and covered to the east by piedmont sediments. It can be divided into three areas: 1) The eastern sector, with low deformation, characterized by S_1 penetrative foliation, with predominantly northeast strike and westward dip, visible in metapelites, 2) the central sector, moderately deformed and

strongly foliated, and 3) the western sector, located on the boundary with the Villavicencio fault system, where deformation is intense, with strong planar fabrics and isoclinal folds (Giambiagi et al., 2011). The LPC intrudes into the eastern low-deformation domain.

4. Results

4.1. Petrography of the La Peña Complex (LPC)

The facies of the LPC were initially described by Mezzeti (1968), better defined by Villar and Zappettini (2000), and recently by Zappettini et al. (2013) who grouped them into two plutonic facies (pyroxenite core surrounded by a malignite–borolanite association) and a system of radial and annular dikes (trachytes, tephrite to phonolite, alkaline lamprophyres and intermediate varieties, porphyritic microledmorite, benmoreite and alkaline trachyte, and a swarm of ouachitite dikes, trachytic to phonolitic volcanic necks). Ouachitite dikes and trachytic to phonolitic volcanic necks occur outside our study area.

In this study we perform the petrographic description of the main or volumetrically more important facies and show and document new and different petrographic details.

We recognize that the clinopyroxenite is constituted by a cumulate facies and a system of mafic dikes that cross-cut it. It occurs in several, partially discontinuous outcrops interpreted to correspond to a single body that covers an area of approximately 2 km^2 in the eastern and southern part of the complex. This clinopyroxenite body is intruded by a central syenite facies that produces, on its margins and primarily in the southern sector, a dense network of veins and conduits, with development of a large breccia zone where syenite material is abundant and causes mechanical disintegration of the clinopyroxenite. These plutonic facies are intruded, preferably in the northern part of the complex, by trachyte and syenite porphyry necks from which radiates a system of dikes of trachyte composition and thin late mafic dikes (Lmd) with which they locally have complex cross-cutting relationships.

A malignite (melanocratic nepheline syenite) cropping out in the eastermost part of the LPC, petrographically and geochemically different from the other syenites, was assumed as representing a primary and initial plutonic facies (Villar and Zappettini, 2000; Zappettini et al., 2013).

Based on our survey (Fig. 1C), the LPC is composed of several intrusions, predominantly plutonic, with subvolcanic facies represented in lower volumes. These can be mainly grouped into: (1) a clinopyroxenite body with facies of cumulate clinopyroxenite (Cc), (2) early mafic dikes (Emd); (3) isolated malignite bodies; (4) a central syenite intrusive with facies of foid-bearing syenites, foid syenites and monzosyenites producing an intrusive breccia at the contact between clinopyroxenite and syenite; (5) trachyte and syenite porphyry necks and a system of radial and annular dikes.

4.1.1. Cumulate clinopyroxenite (Cc)

The cumulate facies is a clinopyroxenite with mid-to-coarse grained texture of adcumulate type, locally micropegmatoid. It essentially consists of clinopyroxene with accessory amounts of biotite, apatite and ore minerals (Ti-magnetite with exsolutions of ilmenite and ulvospinel). The clinopyroxene is diopside, as it was previously identified by Villar et al. (2002), and occurs in 2–30 mm long subhedral individuals, slightly zoned. Biotite is locally abundant and occurs as anhedral interstitial grains. Ore minerals are also interstitial, crystallized after clinopyroxene and biotite, and occasionally form thin lenses. Apatite is abundant included in clinopyroxene, biotite and ore minerals, it is rarely interstitial. It also occurs like late acicular crystals, filling veins up to 0.5 mm. In the clinopyroxenite thin gabbroic pegmatite dikes (5–50 cm) were locally recognized, as well as K-feldspar intercumulus, and veinlets and irregular spaces filled with zeolites.

4.1.2. Early mafic dikes (Emd)

The entire cumulate is cross-cut by mafic dikes, usually a few centimeters thick, but exceptionally a few meters thick, which are confined to the clinopyroxenite body; the larger dikes exhibit diffuse and irregular contacts. Their grain size is fine to very fine and their structure is fluidal. It was recognized a microporphyrytic variety which consists of clinopyroxene and apatite microphenocrysts in a groundmass of plagioclase microlites, subordinate K-feldspar, abundant titanomagnetite and scarce interstitial biotite. Some varieties are accumulations of clinopyroxene microphenocrysts with interstitial feldspar or ore minerals.

4.1.3. Malignite facies

The malignite facies crops out as small isolated bodies on the eastern boundary of the complex, bordering the clinopyroxenite. It is discordant to the metasedimentites of the Villavicencio Formation, developing a thin contact aureole ($\leq$0.8 m). Locally, this facies is intruded by syenites, and trachyte dikes. The malignite contains a few small xenoliths (<5 cm) of fine-grained clinopyroxenite. In the southern outcrop, the malignite locally intrudes the hosting coarse-grained clinopyroxinite, developing a breccia of metric thickness. This is a heterogeneous rock, of inequigranular poikilitic texture, middle-to-coarse grained, consisting of K-feldspar encompassing nepheline crystals and clinopyroxene glomeruli, amphibole, garnet (*melanite*), titanite and, as accessories, sodalite, abundant biotite and ore interstitial minerals. Secondary minerals as zeolites, calcite, fine-grained muscovite and possibly cancrinite replace foids and also occur as veinlet fillings and irregular pegmatite differentiates. An external unit (EU), approximately 1.20 m in thickness, occurs with flow structure and seriate microporphyritic texture. It consists of a network of microphenocrysts of K-feldspar, nepheline, plagioclase and occasionally amphibole, with interstitial alkaline groundmass of feldspar and nepheline, along with subordinated garnet (*melanite*), amphibole and sodalite. Scarce biotite, clinopyroxene, titanite, apatite and disseminated and interstitial ore minerals were recognized as accessory minerals.

4.1.4. Central syenite

The central syenite intrusive covers a large area of the complex and its contacts with the Villavicencio Formation are rarely exposed due to the extensive colluvial cover. On satellite images and few outcrops straight and high-angle contacts were observed (subvertical or 65°–80° inwards). On the western border, the central syenite is concordant with the stratigraphy of the country rock and the remaining contacts are not concordant but controlled by fractures. In contact with the clinopyroxenite, it develops an extensive breccia zone. We petrographically identified syenites, foid-bearing syenites, foid syenites and monzosyenites. The structure is normally fluidal. Overall, they present seriate to seriate microporphyritic texture and, occasionally, grained seriate texture. They consist of K-feldspar, nepheline, amphibole, clinopyroxene, garnet (*melanite*), titanite and ore minerals. Foid monzosyenites and foid-bearing syenites are characterized by their plagioclase content. Locally, pseudoleucite crystals were identified in these facies. In microporphyritic varieties, tabular K-feldspar and plagioclase phenocrysts are oriented in conjugate planes, forming a network of crystals that develop triangular interstitial spaces occupied by a fine-grained alkaline groundmass (K-feldspar and nepheline). Occasionally, small garnet crystals, partially reabsorbed by amphibole, crystallize in interstices. Plagioclase crystals with oscillatory optical zoning and reaction rims of K-feldspar (anti-rapakivi texture) and

garnet with irregular and oscillatory optical zoning are frequent. Zeolites are abundant, accompanied by epidote and possible cancrinite, forming a combination of deuteric alteration that replaces the groundmass and, partially, the primary nepheline, K-feldspar and plagioclase crystals.

4.1.5. Intrusive breccia

The intrusive breccia occurs at the contact between the clinopyroxenite and syenite and covers an extensive area, mostly along the west and northwest borders of the clinopyroxenite body. On the basis of the matrix proportion and the morphology of incorporated fragments it is internally heterogeneous. It is composed mostly of fragments and blocks of cumulate clynopyroxenite; in lower proportion participate fragments of Emd, locally fragments of grabbroic pegmatite dikes, and very occasionally of malignite. The breccia fragments are embedded in a syenite matrix of seriate microporphyritic texture and flow structure and consist of plagioclase and K-feldspar microphenocrysts, with subordinate amounts of amphibole and clinopyroxene arranged in a fine-grained K-feldspar groundmass.

4.1.6. Porphyry necks

The porphyry necks form small bodies, normally elliptical to slightly circular and occur in the central part of the complex. They generally display sharp contacts, but in occasions they can be diffuse. Their distinctive coloration is yellowish-red given by the alteration of iron minerals. They show significant texture variations, from strongly porphyritic to seriate fine- and coarse-porphyritic; flow-oriented crystals are common. In the central zone of the LPC, the main neck shows a brecciated internal structure, with abundant xenoliths or fragments of clinopyroxenitic and syenitic compositions and trachytic autoclasts, partially oriented in the flow direction. Compositionally they can be classified as syenite and trachyte porphyries. They consist basically of K-feldspar and plagioclase phenocrysts and microphenocrysts, accompanied by clinopyroxene, titanite, apatite and occasionally sodalite and garnet (*melanite*). The phenocrysts are normally immersed in a trachytic groundmass in the trachyte porphyries, or in a grained seriate groundmass in the syenite porphyries.

4.1.7. System of dikes

The radial and annular dikes, intruding into the plutonic facies and into the Villavicencio Formation, are apparently cogenetic with the trachyte and syenite necks from which they radiate. Overall, they present variable thicknesses, 0.20–10 m, and some exhibit remarkable chilled borders. These dikes are composed of foid-bearing trachytes, feldspar trachytes and, less frequently, syenite and are intruded by thin Lmd. They are porphyritic and exhibit marked fluidal structure. They are primarily constituted by plagioclase and K-feldspar phenocrysts, accompanied by amphibole, clinopyroxene, titanite, garnet and ore minerals, all arranged in a groundmass of feathery habit and flow-oriented K-feldspar microlites (trachytic groundmass). The foids are sodalite and less frequently nepheline, partially replaced with zeolites, pseudoleucite is present in some facies as large phenocrysts. Secondary minerals are: epidote, calcite, zeolites, clorite, quartz and possible cancrinite; they normally occur as fillings of amygdules or replacing the groundmass and the primary phenocrysts.

The Lmd have a thickness of 10–80 cm; they intrude into all facies displaying complex cross-cutting relationships with trachyte dikes at local scale. They are microporphyritic to porphyritic and display flow structure. They consist of biotite, clinopyroxene and apatite microphenocrysts arranged in a partially altered fine-grained groundmass, formed by K-feldspar, subordinate zeolites and mafites. Disseminated ore minerals, apatite crystals, calcite, zeolites and chlorites were recognized as secondary minerals. They differ from the previously described Emd by their petrography, chemical composition and cross-cutting relationships with all units, and by their radial distribution in association with the trachyte dikes. Temporal relationships between Lmd and Emd are well established because the latter are present in the clinopyroxenite fragments of the intrusive breccia and not in the other rocks, that suggests their early nature in relation to the Lmd that intrude even into the trachytes.

4.2. Morphology and internal structure

4.2.1. Structural analysis of the La Peña Complex (LPC)

Based on the morphostructural design of the complex characterized by different intrusions, apparently centered, it would be normal to expect that the foliation traces in the body will adapt to the contacts between the different units, as occurs in other alkaline complexes or in centered igneous bodies in general. Nevertheless, the internal magmatic structure (Fig. 1C) shows planes striking NNW-SSE, perpendicular to the contacts between the units and very noticeably between the clinopyroxenite and the central syenite. This means that the flow planes run perpendicular to the host rock stratigraphy, except in the southern and western margins of the syenite, where they become locally subparallel. This structural pattern is defined by: a) the preferential strike and flow foliation of the mafic dikes that intrude into the clinopyroxenite, b) the foliation planes in the central syenite and in porphyry necks, c) the strike of some veinlets and syenite conduit in the clinopyroxenite, and d) the preferential strike of trachyte dikes. The only identified lineations in the LPC occur in the central syenite body (Fig. 1C). The internal northwest-southeast structure coincides with a remarkable fracture system present in the host rock and in the clinopyroxenite body (Fig. 1C), denoting that there has been a strong structural control in the emplacement of the magmatic units.

4.2.2. Brittle country rock structures

The LPC lies on the eastern part of the Villavicencio Formation, within the eastern structural domain of the Precordillera. The country rock is affected by a system of discontinuities related to a brittle shear zone cropping out about 500 m east of the intrusive (Fig. 1C). Shear occurs on discrete planes striking N–S to N20 W and dipping 80°–85° E and ENE (Fig. 2A, B and Fig. 3A) that coincide with the stratification of the country rock in that sector. Whereas, to the west of the complex it could correspond with a deformation zone associated to the Villavicencio fault system (Fig. 1B). In this area, the Villavicencio Formation is characterized by alternation of metasandstone and pelite beds, which show differential rheological behaviors in response to deformation. Fine-grained lithologies are used as take-off areas, whereas thicker competent beds develop fractures and dilatant spaces (Fig. 2C). Fault planes exhibit cataclasis with development of fault soapstone (Fig. 2A1), and kinematic indicators on shear planes (fault grooves and steps) show sinistral, normal-sinistral and sinistral-normal motion, with a northward rake of 15°–50°, respectively (Fig. 2A2 and B1). The fracture systems identified in the country rocks can be defined as Riedel (R), Anti-Riedel (R′) and extensional (T) fractures, on the grounds of their kinematic features and their angular positions relative to the main shear (Fig. 2B and D). In addition, a synthetic system is recognized principally in the southwestern area of the magmatic breccias, with a trend ranging from N50°E to N60°E and with subvertical dips and sinistral motions. They are interpreted as discontinuities systems (P).

4.2.2.1. Riedel systems. The recognized synthetic Riedel (R) shears (Fig. 2C and D) show strikes ranging from N10°W to N30°W, they

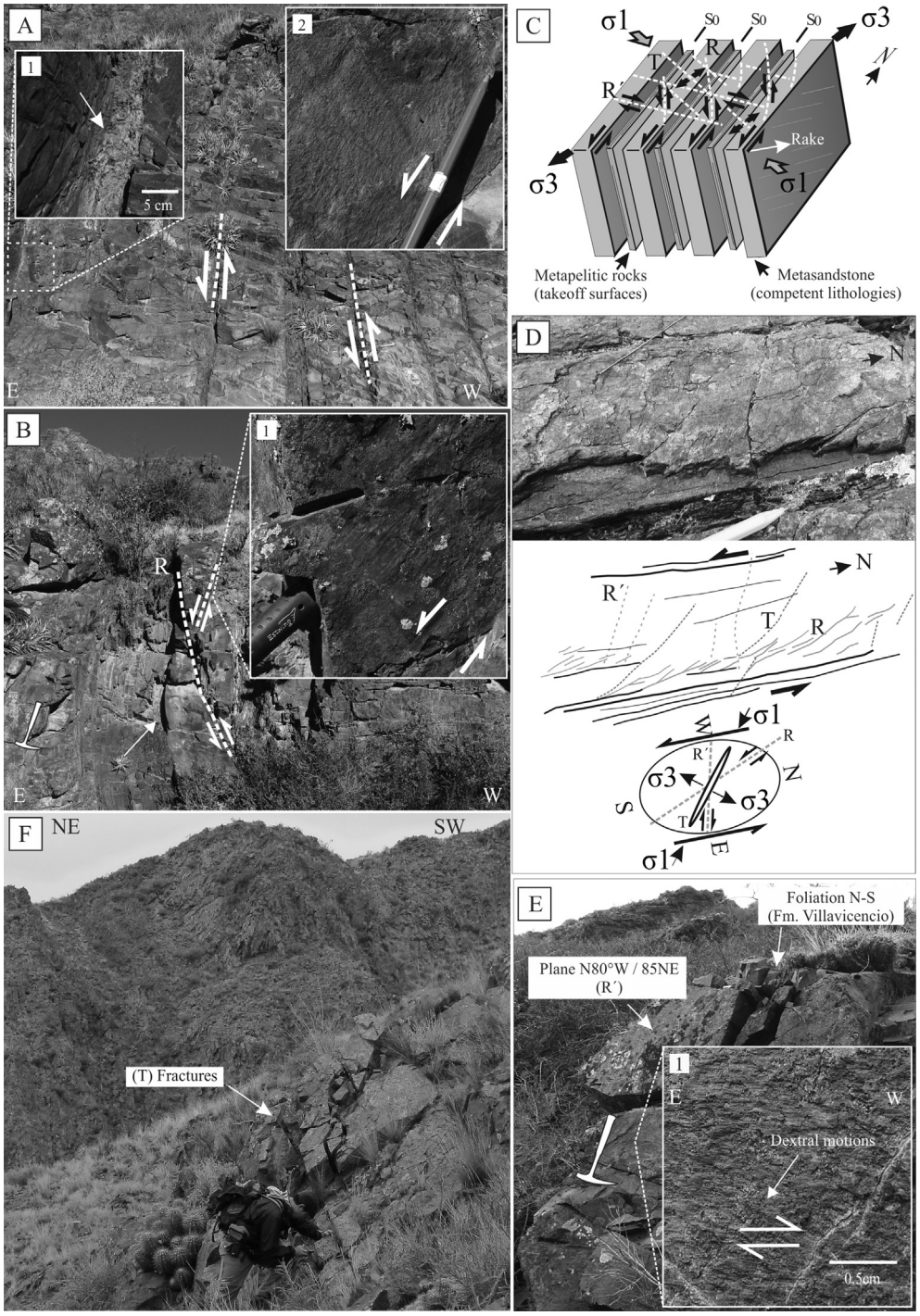

Fig. 2. Shear zone and associated structures developed in the Villavicencio Formation. A) Discrete shear planes in less competent fine lithologies, and details of the shear planes showing fault soapstone (1) and friction grooves (2). B) Riedel fractures cross-cutting the foliation of the Villavicencio Formation and producing deformation by folding on adjacent beds (white arrow) and (1) detail of a shear plane showing grooves with northward rake of 50° and normal-sinistral motion. C) 3D scheme of the shear zone with stress relationships. D) Photograph of a shear affecting a metasandstone bed and a graphic representation of the fracture system and its relationship with stress. E) E–W plane (R′) with detail of grooves (1). F) NW–SE extensional fractures.

are subvertical and normally incline 75°–85° to WSW, with their angles to the shear planes ranging 10° and 25°.

Antithetic Riedel shears (R′) (Fig. 2D and E) are obliterated by widely distributed joints, with similar attitudes, which hinders their recognition and measurement. The strike of identified planes varies between N75°W and N85°W, with dips of 85° to the NE and 80° to the SW; their angles to the shear plane are about 75°–80° and the striations on the fault plane define dextral motion (Fig. 2E1).

4.2.2.2. Extensional fractures (T). Extensional fractures (T) (Fig. 2D and F) are widely distributed over the whole country rock, but mainly in the vicinity of the intrusive where massive sandstone beds crop out. They strike N40°W to N65°W and occasionally

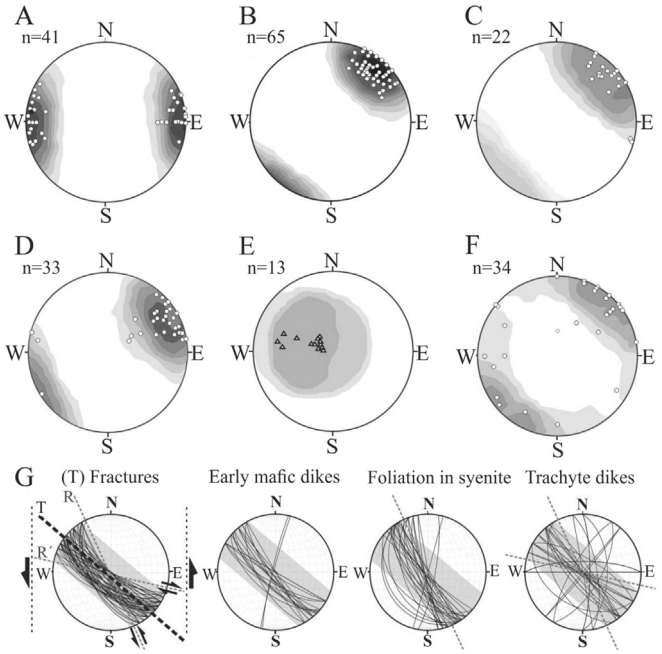

Fig. 3. Stereographic representations of structures in the area, projection of poles: A) Stratification of Villavicencio Formation; B) Distension fractures; C) Foliation in Emd; D) Foliation in syenite; E) Lineation in syenite; F) System of trachyte dikes. G) Projection of planes and comparison of NW–SE distension fractures (shaded area) with magmatic fabric of the LPC. Note the coincidence between extension (T) and magmatic structures.

N30°W, with 60°–85° SW and sometimes subvertical dip (Fig. 3B). They normally keep angles of 50°–35° with respect to the main shear planes. These extension fractures are also observed in the clinopyroxenitic rocks.

4.2.2.3. Subordinate systems of fractures. A different system of discontinuities striking NW and N10°W and dipping 65°–70° E–NE is observed in the country rock, at the contact with the malignite facies. These discontinuities are parallel and sub-parallel to the internal foliation of the magma unit and develop plane contacts with it.

4.2.2.4. Kinematic analysis of shear. The kinematic indicators identified in the shear zone reflect extensive motions with strike component and strike motions with a certain extensional component, indicating an overall divergent local tectonic setting (transtension). In addition, we used the geometric method performed by McCoss (1986) to elucidate whether the genesis of structures responds to transtension zones as revealed by field evidence.

The simple McCoss's geometric reconstruction (1986), which is based on a modification of the model by Sanderson and Marchini (1984), allows a fast determination of the main axes of the infinitesimal strain ellipsoid orientation and provides a simple graphic solution to discriminate between transpressional and transtensional zones. In this context, it is necessary to determine the angle of infinitesimal displacement direction ($\hat{A} = 180° - 2W$), with W being the angle formed between extensional fractures and the shear plane that contains them, which is graphically defined (Fig. 4). In the LPC, the average value of $\hat{A}$, determined exactly in the shear zone, is 101°, indicating that it is a transtension system near the boundary of the simple shear zone, where $\hat{A}$ is 90° (Peacock and Sanderson, 1995), showing the compatibility with the field evidence.

4.2.3. Internal structure, magmatic fabric

4.2.3.1. Clinopyroxenite. The coarse facies of the clinopyroxenite body is adcumulate and its stratification is not clear. The entire massif is affected by NW–SE extensional fractures (Fig. 5A), into which intrudes an important fraction of Emd (Fig. 5B and C). The internal planar fabric of dikes is sometimes identified at mesoscopic scale (Fig. 5D) and other times only microscopically (Fig. 5E and F). The flow planes are defined from the orientation of the clinopyroxene microphenocrysts and plagioclase microlites in the microporphyritic varieties (Fig. 5E) or from the orientations of clinopyroxene crystals accumulated in the border of the dikes (Fig. 5F). The internal planar fabric is parallel and subparallel to the border of the dikes and coincides with their overall strike. Although internal flow lines and dikes generally strike N30°W, N55°W to N65°W with vertical, subvertical and 80 to 60° inclination toward the SW (Fig. 3C), others display different orientations principally N50°E. Microstructural evidence denotes that minerals of the fluidal facies are oriented parallel to the borders of the adcumulate or surround incorporated xenoliths.

4.2.3.2. Malignite facies. The fabric of the malignite facies (Fig. 6A) can be divided into an internal unit (IU) and an external unit (EU) (Fig. 6B). This facies is discordant to the metasedimentites of the Villavicencio Formation, according to sharp, straight contacts (N10°W and N–S) and strongly dipping contacts of 60°–75° towards the ENE, concordant with a local fracture system (Fig. 6A, C and D). The planar fabric is clearly defined in the EU and absent or weak in the IU. The IU is generally massive, although it sometimes exhibits slight traces of foliation, outlined by veinlets and pegmatite differentiates (Fig. 6E), parallel and subparallel to the contacts with the host rock. Intrusive autobreccias are observed in the EU composed of strongly rounded and rotated fragments (Fig. 6F). In the EU, the flow structure is defined by the preferential orientation of the microphenocrysts and phenocrysts of plagioclase, K-feldspar, nepheline and amphibole prisms. The foliation is N10°W and N–S with 60°–75° inclination toward the ENE, parallel to the contact (Fig. 6A). The lineations could not be determined because of the poor preservation of the outcrop. Microscopically, the border facies present families of conjugate planes (Fig. 6G) composed of aligned K-feldspar and nepheline crystals. The oblique planes create triangular interstitial spaces (pressure shadows) where a fine K-feldspar and nepheline groundmass crystallizes, sometimes accompanied by amphibole and *melanite*, where it is frequent that *melanite* crystals adapt their morphology to the geometry of the interstices (Fig. 6G). There were also recognized K-feldspar phenocrysts with irregular extinction (Fig. 6H) and fractures in nepheline and plagioclase crystals filled with K-feldspar from the groundmass (Fig. 6I and J).

4.2.3.3. Central syenite. The intrusion of the syenite body produces an extensive breccia zone at its contact with the clinopyroxenite (Fig. 1C). The areas adjacent to the contact are characterized by a dense network of leucocratic veinlets and syenite conduits that locally show a NW–SE trend (Fig. 7A). The intermediate zones show dismembered xenoliths and clinopyroxenite angular blocks incorporated into an abundant syenite matrix (Fig. 7B). The rounded, partially reabsorbed xenoliths, that become in *schlieren* oriented along flow lines (Fig. 7C), are common in zones remote from the contact, or in zones with higher percentage of syenite matrix. Locally, in the breccia zone near the clinopyroxenite, occur dikes or conduits with NW–SE trend, formed by angular to subangular clinopyroxenite fragments arranged in a syenite matrix (Fig. 7D). The structural features of the breccia reflect different fragmentation stages, dismembering and reabsorption of the clinopyroxenite blocks and fragments, exemplified in Fig. 7E. Although the inner

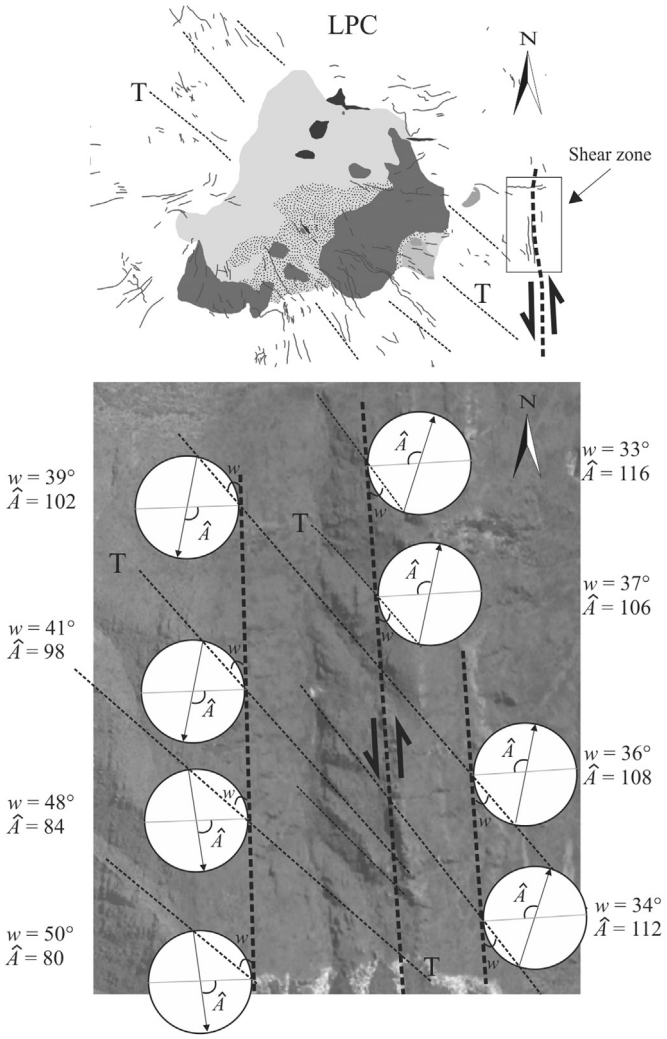

Fig. 4. Geometric method McCoss (1986), realized on Google Earth images obtained by Stitch Maps software; the image correspond to the shear zone, western of the LPC, where were identified the extensional fractures and measured the angles between these and the shear zone. Â: angle of infinitesimal displacement, obtained using the formula ($Â = 180° - 2W$); *W*: angle formed between extensional fractures and the shear plane that contains them and is graphically measured angle. The average determined value of Â is 101°, indicating that it is a transtensional system near the boundary of the simple shear zone, where Â is 90°.

breccia pattern is heterogeneous, locally a great number of veinlets and breccia conduits are aligned along a NW–SE direction, subparallel to the system of extensional fractures of wide distribution in the clinopyroxenite and metasedimentites host.

The fabric of the intrusive body of the central syenite (Fig. 7F) is well defined in the dismemberment zones of the clinopyroxenite blocks (Fig. 7B) and in the outer syenite zone away from the breccia (Fig. 7C). In dismemberment zones it is mainly resolved by the orientation of the fragments (xenoliths) and clinopyroxenite angular blocks which locally are partially absorbed by the syenite magma. In these zones, traces of foliation surround the clinopyroxenite fragments (Fig. 7E3). The foliation in the syenite is defined by the preferential orientation of the K-feldspar, plagioclase and clinopyroxene. In the external part of the syenite, foliation lines coincide with the stretching direction of xenoliths and schlieren. In general, the fabric strikes N15°W to N40°W and it is vertical, subvertical or normally inclined from 80° to 65° SW and 85° towards the NE (Fig. 3D). At the few outcropping points of the western contact, it is parallel and subparallel to the stratigraphy of the country rock. The lineation in the syenite, when it can be measured, normally inclines towards the NW (~80°–70°) (Fig. 3E). Microscopically, conjugate planes are visualized (Fig. 8A and B), in which the primary minerals and the fragments of primary minerals are aligned (K-feldspar, plagioclase, nepheline, clinopyroxene), generating triangular interstitial spaces and pressure shadows occupied by K-feldspar and nepheline groundmass (Fig. 8C), sometimes replaced with zeolites. It is common that amphibole and garnet (*melanite*) occupy triangular interstitial spaces (Fig. 8A and B). The tabular K-feldspar crystals normally exhibit irregular undulatory extinction (Fig. 8C and E) and microfractures filled with groundmass material (Fig. 8D and E). Clinopyroxenite microxenoliths oriented along the flow, surrounded by phenocrysts subparallel to the borders were also identified; plagioclase crystals with disequilibrium textures are common in this unit.

Although the flow plane direction in the syenite is NW–SE, the angles to the main shear are smaller than extensional fractures and closer to the position of the synthetic Riedel shear fracture (R) recognized in the country rock.

In the southwestern sector of the breccia zone, the network veins and the syenite conduit show an apparent chaotic pattern, however, they locally maintain two well-defined trends. In this context, the syenitic veins strike N60°E and N40°W, the first set follows the planes of synthetic shear recognized in the breccia zone, interpreted as (P) systems (Fig. 9A and B) and the second set is closer to the position of the extensional fractures (T) (Fig. 9A). In the area, large syenitic conduits or breccia conduits keep the trend of extensional fractures (T) (Fig. 9C); the intersections between both (P) and (T) systems determine at different scales triangular nodes filled with syenite (Fig. 9D).

4.2.3.4. Porphyry necks. The magmatic structure of these bodies is subparallel to the internal fabric of the syenite. It strikes N50°W to N30°W with subvertical dips and up to 45° to the SW. At microscale, the plagioclase crystals show displacement of twin planes and fractures filled with K-feldspar of the groundmass, some K-feldspar phenocrysts show undulatory extinction and are locally affected by synmagmatic shear with generation of open spaces filled with later phases (very fine-grained K-feldspar and ore minerals) (Fig. 8F).

4.2.3.5. Dike system. The distribution of the dikes presents altogether a defined radial and, less frequently, annular pattern. Within this overall framework, the dikes are emplaced with preferential NW–SE, E–W, NE-SO and N–S strikes (Fig. 3F), following the different fracture systems and stratigraphy of the country rock; statistically they are concentrated according to their preferential N40°W to N65°W strikes, consistently with extensional fractures (Fig. 3F, G and Fig. 10A); locally in the outer zone of the LPC, a few subhorizontal annular dikes occasionally occur. The dikes display complex cross-cutting intrusion-retrointrusion (Bergantz, 2000) relationships with Lmd (Fig. 10B and C), which are locally affected by synmagmatic shears produced in the trachytes before their total crystallization, where the shear plane of mafic dikes is filled by the remainder trachyte melt (Fig. 10C). The internal fabric of light-colored dikes is characterized by strong foliation, defined by the orientation of the K-feldspar, plagioclase and amphibole phenocrysts (Fig. 10D), rarely clinopyroxene, and in occasions amygdules filled with deuteric minerals. Overall, the phenocrysts, some of which have been deformed prior to the total crystallization of the magma, are surrounded by the fluidal trachytic groundmass (Fig. 10E).

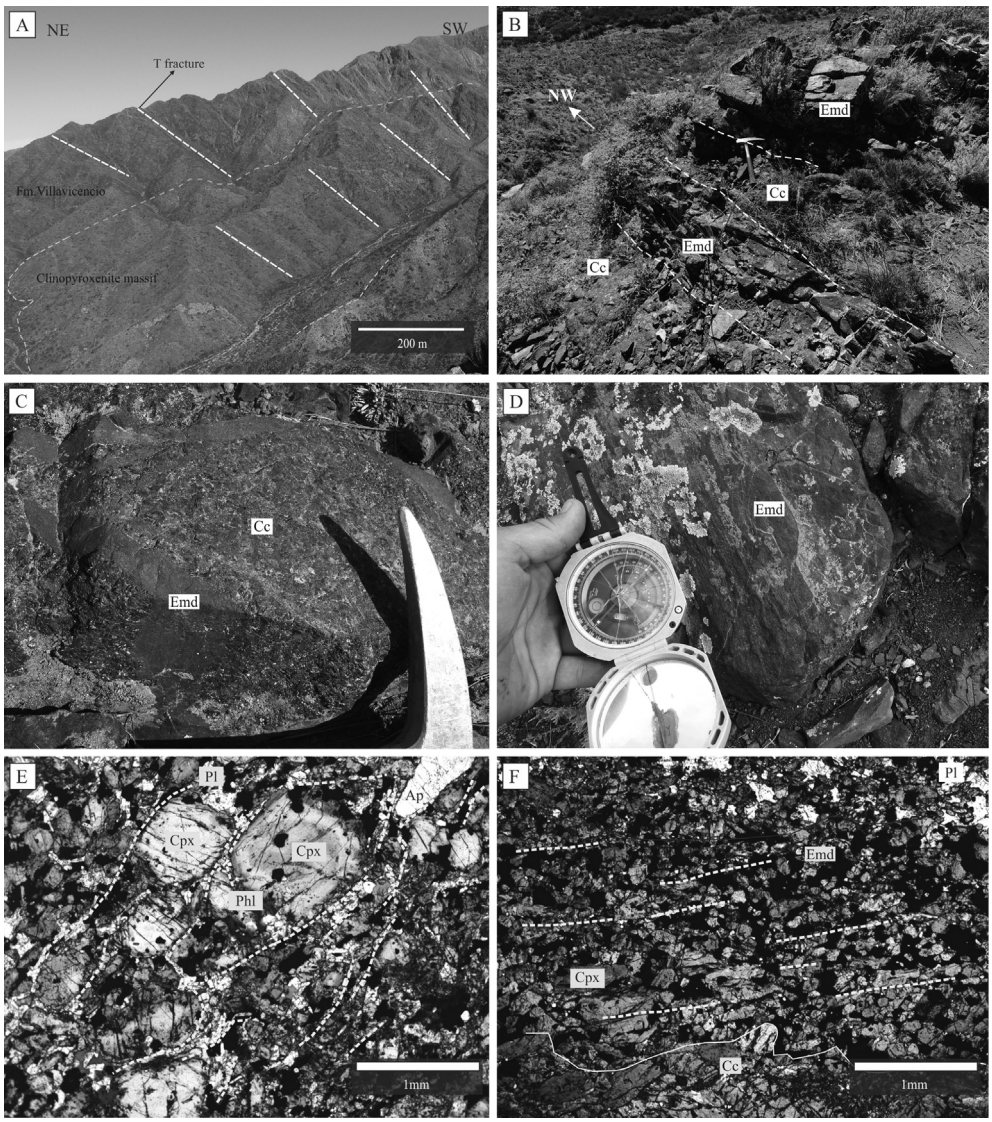

Fig. 5. Structures in the clinopyroxenite. A) Northwest-southeast extensional fractures developed in the clinopyroxenite body and country rock. B) Emd cross-cutting the Cc parallel to the system of extensional fractures (dashed white line). C) Emd intruding into the Cc. D) Foliation in a microporphyry Emd. E) Photomicrography of a microporphyry Emd, dashed lines represent flow traces. F) Photomicrography showing the Cc intruded by an Emd with flow foliation (dashed white lines), the contact is delimited by the white line. Cpx: Clinopyroxene, Pl: Plagioclase, Phl: Phlogopite, Ap: Apatite.

4.2.4. Morphology of the LPC

Although the outline of the LPC has an apparently subcircular design, its real geometry evidenced by the characteristics of the contacts (straight and strongly dipping), responds to a marked control imposed by fractures. It is observed that its western border is concordant with the stratification of the Villavicencio Formation, whereas the remaining contacts are perpendicular to the primary structure of this unit and are conditioned by fractures preferentially NW–SE and locally NE–SW orientation (Fig. 11A), these system of discontinuities define a polygonal form comparable with a triangle (Fig. 11A).

The NW–SE fractures also control the internal fabric of the LPC, as graphically observed in the projections of Fig. 3G, where distension fractures are compared with, and related to, magmatic structures and dikes.

Because of the lack of gravimetric surveys, the morphology and the extension in depth of the LPC are unknown. Nonetheless, taking into account common characteristics of other alkaline complexes, studied and exemplified for different plutons of the province of Kola by Arzamastsev et al. (2000), in conjunction with our observations of the characteristics of the contacts and the subvertical magmatic fabric of the LPC, it is assumed that the morphology at depth could be resolved in a subconical body, with a southwest inclination and straight contacts, constrained by the system of extensional fractures that controls its emplacement and outcropping geometry (Fig. 11B).

4.3. Structural emplacement model

Based on our detailed structural analysis, we propose a structural model that explains the mechanism by which the magma pulses intruded into the crust up to its place of consolidation. For a better understanding of this model we discriminate between both ascent and emplacement mechanisms.

4.3.1. Ascent mechanism

The model proposed responds to brittle deformation processes linked to a shear zone and its network of cogenetic discontinuities,

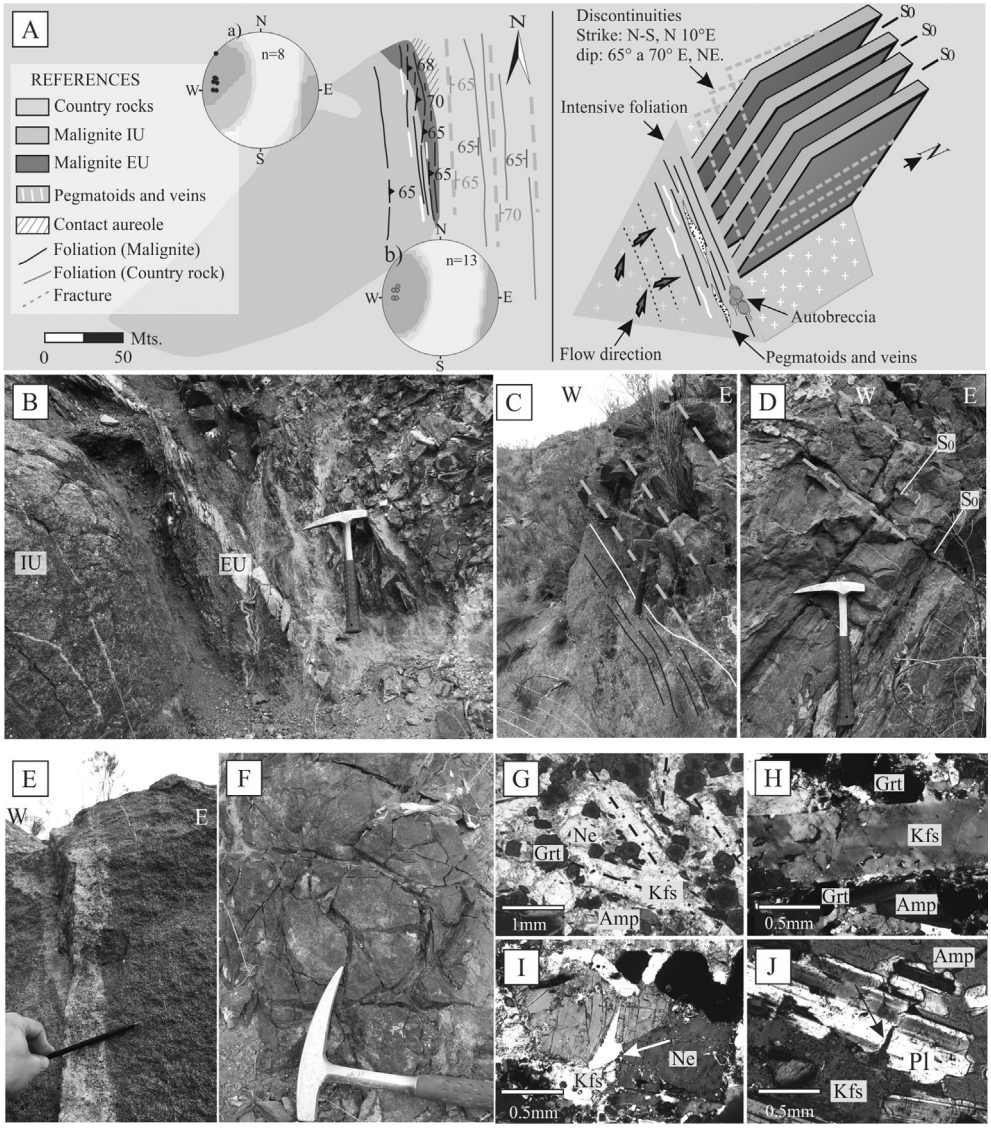

Fig. 6. Malignite facies. A) Structural geological map and 3D representation of the facies, showing internal fabric and relationships with fracture systems, with projections of a) foliation poles and b) fractures. B) Photograph of the IU and EU. C) Contact with the Villavicencio Formation (white line), the foliation traces (black lines) are parallel to the contact, coinciding with an N–S fracture system, N10°W with E and NE dip (dashed grey lines). D) Detail of 6C. E) Pegmatite bands parallel to the foliation. F) Intrusion-autobreccia. G) Photomicrography showing conjugate planes defined by Kfs strike; note the triangular spaces occupied by Grt, whose crystals adapt to interstices. H) Kfs with irregular extinction. I) Ne crystal, and J) Pl crystal, both with fractures filled with Kfs of the groundmass. Kfs: K-feldspar, Pl: Plagioclase, Ne: Nepheline, Amp: Amphibole, Grt: Garnet.

which display angular relationships and present local motions defined by their position with respect to the regional stress field (Fig. 11C). In the area, the stress field can be explained with an ellipsoid constructed by a NE–SW trending σ3 axis and an NW–SE trending σ1 axis (Fig. 11C and D). The shear on the eastern border of the complex develops on discrete planes striking submeridionally, concordant with the stratigraphy of the Villavicencio Formation. It is not clearly defined on the west of the intrusive, but it may correspond to a complex deformation zone near the Villavicencio fault system, characterized by mesoscale faults developing a strike regime with a main north-south shortening direction, assigned to the Permian period (Giambiagi et al., 2011). Due to a lack of timing constrain, these strike-slip structures (first assigned to the Permian strike-slip event) could have been developed later, during the Andean orogeny.

We propose that the shear zone affected the crust, producing a network of discontinuities with a *K*-type fractal fracture pattern, which controlled magma melt migration by an opening in the different branches. This may have occurred particularly in the dilatant zones (T), similarly as indicated by Morosini et al. (2012) for emplacement of volcanic and subvolcanic bodies in La Carolina district, San Luis, Argentina. In this context, the fracture propagation mechanism (Clemens and Mawer, 1992; Petford, 1996) would have facilitated the ascent of different magma pulses possibly derived from one or more deep chambers.

According to Villar and Zappettini (2000) and Zappettini et al. (2013), the first pulse would have a chemical composition close to that of malignite. If so, the outcropping body in the eastern part of the complex might represent such pulse. However, cross-cutting relationships show that it corresponds to a pulse subsequent to the formation of the clinopyroxenite cumulate. Within this context, we propose that the fractionation of a basanitic magma would have caused the formation of the clinopyroxenite cumulate by sedimentation (Fig. 11D); the syenites and trachytes were originated by fractionated crystallization of the same melt from which its original composition is not present, although it might have a bulk

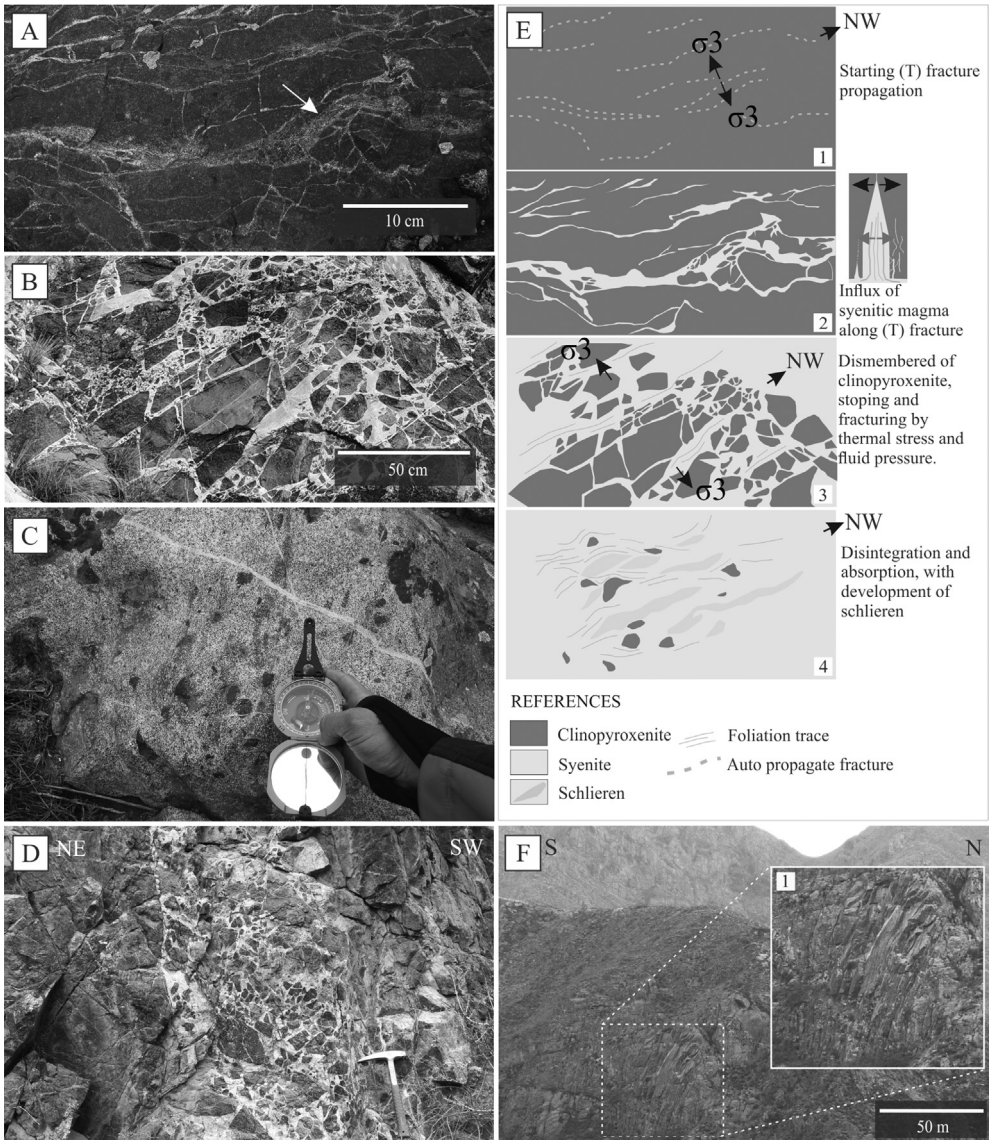

Fig. 7. Internal fabric of the syenite and the breccia zone. A) Veinlets and syenite conduit (white arrow) with NW–SE strike. B) Clinopyroxenite dismembered in angular blocks following the syenitic flow. C) Flow foliation in the syenite, note that some xenoliths are rounded and others reabsorbed. D) Conduit striking northwest-southeast, made up of clinopyroxenite fragments in a syenite matrix. E) Sequence of syenite intrusion into the clinopyroxenite, interpreted from A, B and C, with detail of fracture propagation mechanism (1and 2); fragmentation of the syenite by stoping process, thermal stress and fluid pressures (3), and finally, absorption of xenoliths (4). F) Central syenite and detail of internal foliation planes (1).

composition close to the malignite or alternatively to the Lmd. The second pulse is represented by Emd that cross-cut the clinopyroxenite cumulate preferentially following NW–SE extension fractures (Fig. 11E), whereas the third phase would be represented by the malignite (Fig. 11F). The system of discontinuities that favored the emplacement of Emd would later facilitate the intrusion of the syenite magma, which would have ascent in numerous sheets along the fractures (Fig. 11G). The last intrusive phase is represented by the porphyry necks and the radial and annular dikes (Fig. 11H). The relations between trachyte and Lmd show the interactions of different magmas (minglin-mixing) and the influx of a basic magma into the trachytic magma, likely along different structural levels (Fig. 11H). Radial and annular dikes can be associated with specific stress fields, linked to local magmatic pressures generated by central intrusions (focal point), represented by porphyry necks (Fig. 11H). Although the radial pattern is evident (Fig. 1C, Fig. 3F and G), the great concentration of dikes according to preferential northwest-southeast directions highlights again the importance of extensional fractures (T) in the ascent of each of the pulses.

4.3.2. *Emplacement mechanisms*

At the moment of the emplacement different mechanism would have acted, they are summarized in: 1) opening of discontinuities synchronous to the magma circulation as the principal mechanism for formation of dikes and conduits; 2) stoping processes and physical disintegration of host rocks and 3) regional stress deformations.

It is considered that the magmatic pressures exerted by the different sheets on the walls of the discontinuities (Fig. 7E2) would favor their opening, synchronous to the magma circulation, making effective the ascent and producing dikes and breccia conduits. In addition, the fragmentation of the clinopyroxenite into angular blocks and xenoliths would have been assisted by fracturing of

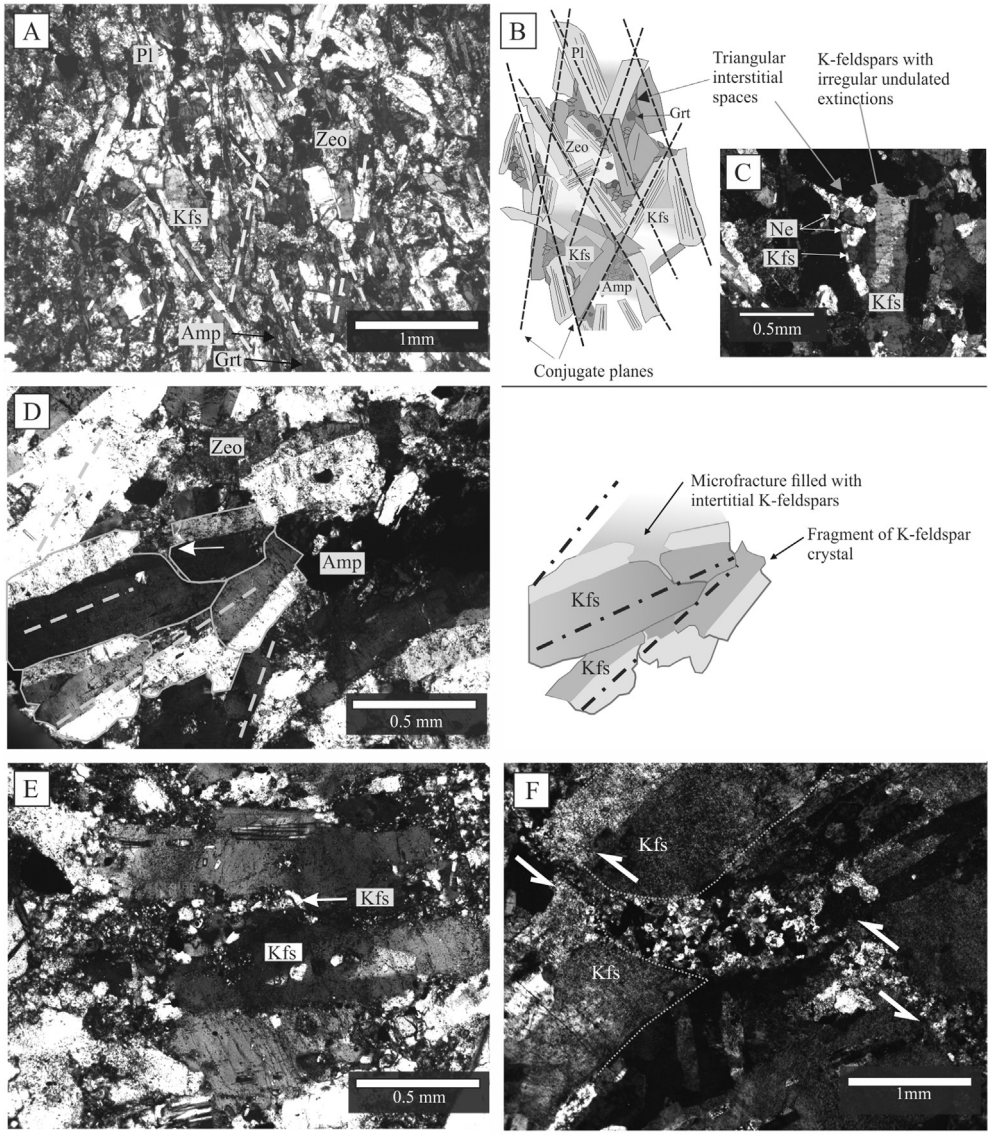

Fig. 8. Internal fabric of the central syenite. A) Conjugate planes (dashed gray lines) in a foid monzosyenite facies, triangular interstitial spaces are observed among primary minerals. B) Representative graphic of conjugate planes in a foid monzosyenite; note the triangular spaces occupied by Kfs, Amp and Grt. C) Interstitial spaces with feldspar and nepheline matrix. D) Kfs crystal exhibiting deformation with development of wedges filled with groundmass material. E) Kfs crystals exhibiting intracrystalline deformation with development of wedges filled with groundmass material (white arrow). F) Synmagmatic shear in a syenite porphyry. Kfs: K-feldspar, Pl: Plagioclase, Ne: Nepheline, Cpx: clinopyroxene, Amp: Amphibole, Grt: Garnet, Zeo: Zeolite.

both, mechanical and thermal mechanisms; these processes involve stoping (e.g., Pinotti et al., 2002; Žák et al., 2006), fragmentation by thermal stresses (Daly, 1903; Marsh, 1982; Furlong and Myers, 1985; Clarke et al., 1998; Pignotta and Paterson, 2007) and fragmentation by excesses of the fluid pressure or hydraulic fracturing (Clarke et al., 1998); the disintegration of the blocks prepares the rocks for assimilation by combinations of mechanical dispersions and chemical reactions. These mechanisms play an important role in the development of the breccia zone, and enabling an efficient transference of material during the emplacement of the magma (Buddington, 1959; Marsh, 1982; Furlong and Myers, 1985; Paterson et al., 1996; Yoshinobu et al., 2003).

Graphically, these processes are represented in Fig. 7E, which subsequently indicates: 1) initiation of the fracture propagation, 2) emplacement of the veinlets and development of the breccia conduit, 3) fragmentation of the clinopyroxenite into xenoliths, and 4) disintegration and reabsorption of the clinopyroxenite xenoliths with consequent contamination of the syenite.

Finally, the deformation acting on the different magma pulses is evident in the central syenite body, where deformation processes caused by shearing are recorded at microscale, with development of families of conjugate planes (proto-shears) (Fig. 8A and B). The internal structure of the syenite would then be the combination of: 1) intrusion through dilatant zones and 2) synchronous deformation associated to shearing, which acts on the multiple magma sheets at an advanced stage of crystallization.

5. Discussion

5.1. Ascent and emplacement

The relationships and interactions between faulting and magmatism and the importance of faulting in magma emplacement have been largely discussed and studied for the emplacement of granite magmas associated with transcurrent zones (Guillet et al., 1985; Hutton and Reavy, 1992; D'Eramo et al., 2006), extensional

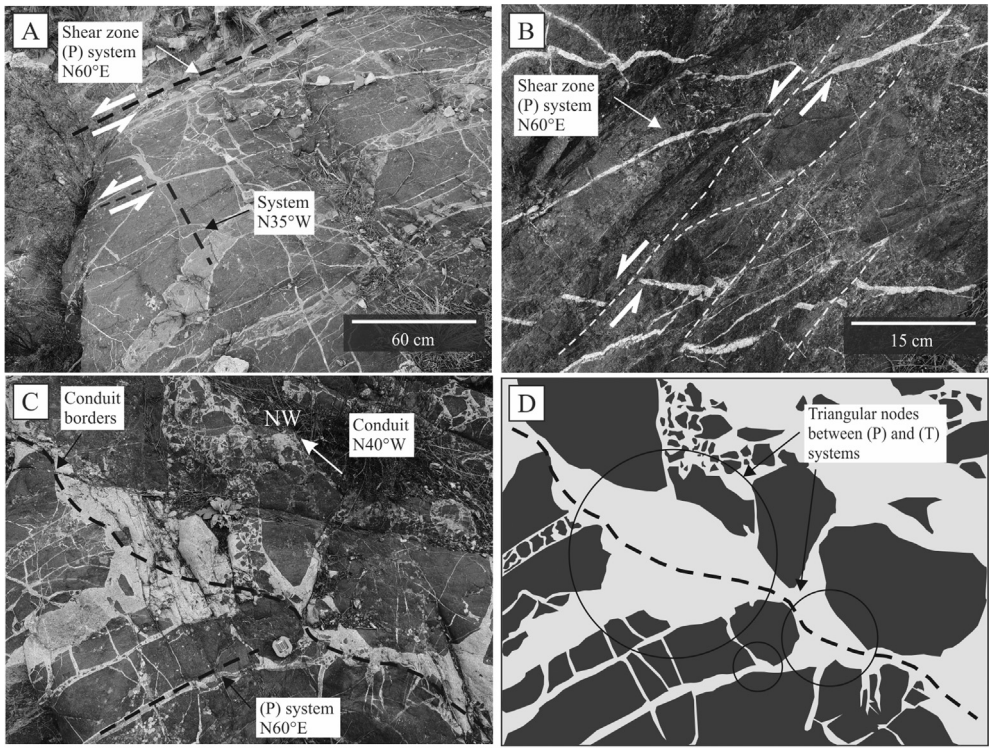

Fig. 9. Southwestern sector of the breccia zone. A) Veins network and syenite conduit show two well-defined trends; syenitic veins strike N60°E and N35°W, the first along of the planes of synthetic shear, interpreted as (P) and the second closer to the position of the extensional fractures (T). B) (P) synthetic shear, affecting clinopyroxenite. C) Syenitic conduits keep the trend of extensional fractures (T); note the intersections between both (P) and (T) systems, determine at different scales, triangular nodes filled with syenite. D) Detail of 9C.

zones (Hutton et al., 1990; Bouillin et al., 1993) and contractional zones (Tobish and Paterson, 1990). In relation to alkaline magmas, cortical guidelines and associated faults in rift environments normally control their intrusion, even generating intrusion provinces, as happens in the east of Africa (Le Bas, 1977; Bell and Blenkinsop, 1987a), south of Brazil (Morbidelli et al., 1995), Greenland (Nielsen, 1980; Larsen and Rex, 1992), east of the Canadian shield (Bell and Blenkinsop, 1987b), Kola peninsula, Russia (Kogarko et al., 1995) or in the Monchique complex, Portugal, where its emplacement from the upper mantle was favored by the existence of crustal fractures (Valadares and González-Clavijo, 2004). It is evident that fractures act as conduits and generate spaces for ascent of magma within the continental crust (Dehls et al., 1998; Petford et al., 2000). The LPC represents a clear example where the ascent of the different pulses at shallow crustal levels is clearly controlled by the fractures that finally constrain their morphology. In addition, strike slip shear zones would have also favored the circulation of melts in the study area, as seen in the SSW sector of the breccia zone, where numerous syenitic veins follow directions of the synthetic shear plane (P) (Fig. 9). In this context, the dynamic interactions between both flow and faults allowed the circulation or migration of the fluid, as suggested Sibson (1990, 1996 and 2000). During the emplacement of the LPC, other mechanisms would have play an important role, that is, stoping, magmatic stress and regional stress. Stoping process (e.g., Daly, 1903, 1933; Pinotti et al., 2002; Žák et al., 2006; Pignotta and Paterson, 2007) involves the dislodgement of pieces of the host rock (stoped blocks) by magma, and subsidence (or ascent) of included blocks; the mechanisms linked to stoping, fracturing by thermal stress and fluid pressures, would have favored the fragmentation of the clinopyroxenite in angular blocks and xenolits allowing the development of the magmatic breccias and the transference material during the emplacement of the magma (Buddington, 1959; Marsh, 1982; Furlong and Myers, 1985; Paterson et al., 1996; Yoshinobu et al., 2003).

The polygonal form of the LPC and its internal structure indicate that ascent of the magma is controlled by a system of discontinuities principally NNW-SSE (Fig. 11A). The coincidence of magmatic fabrics with contemporary structures of the host rock denotes a strong tectonic control during formation of the complex, which can be related to a brittle shear zone that would favored the emplacement and affected, locally, its internal fabric. On the other hand, the nearly subcircular design and the system of radial and annular dikes shown by the LPC are morphostructural features that suggest an important stress field produced by magmatic pressures (magmatic stress).

The activity of the structure responsible for the emplacement also affects the microfabric of the central syenite intrusive and can be explained by shearing on a magma with a considerable proportion of crystals, which results in the development of conjugate planes and ultimately produces “submagmatic flow” (Vernon, 2000). In this context, deformation on the magmatic *mush* of syenite composition produces undulatory extinction in primary crystals and microfractures filled with late magmatic phases, mainly represented by feldspar and nepheline groundmass sometimes accompanied by *melanite* and amphibole. The late magmatic material, crystallized in pressure shadows or in zones between fragmented primary grains (Gapais and Barbarin, 1986; Paterson et al., 1989), indicates solid-state deformation in the presence of melt migration. Bouchez et al. (1992) and de Saint Blanquat and Tikoff (1997) suggest that plagioclase fractures filled with quartz and/or K-feldspar indicate submagmatic flow. Vegas et al. (2007), in their structural analysis of synkinematic granitoids from Sanabria, Macizo Ibérico, intruded under transpressive conditions, observed development of conjugate planes through which primary materials

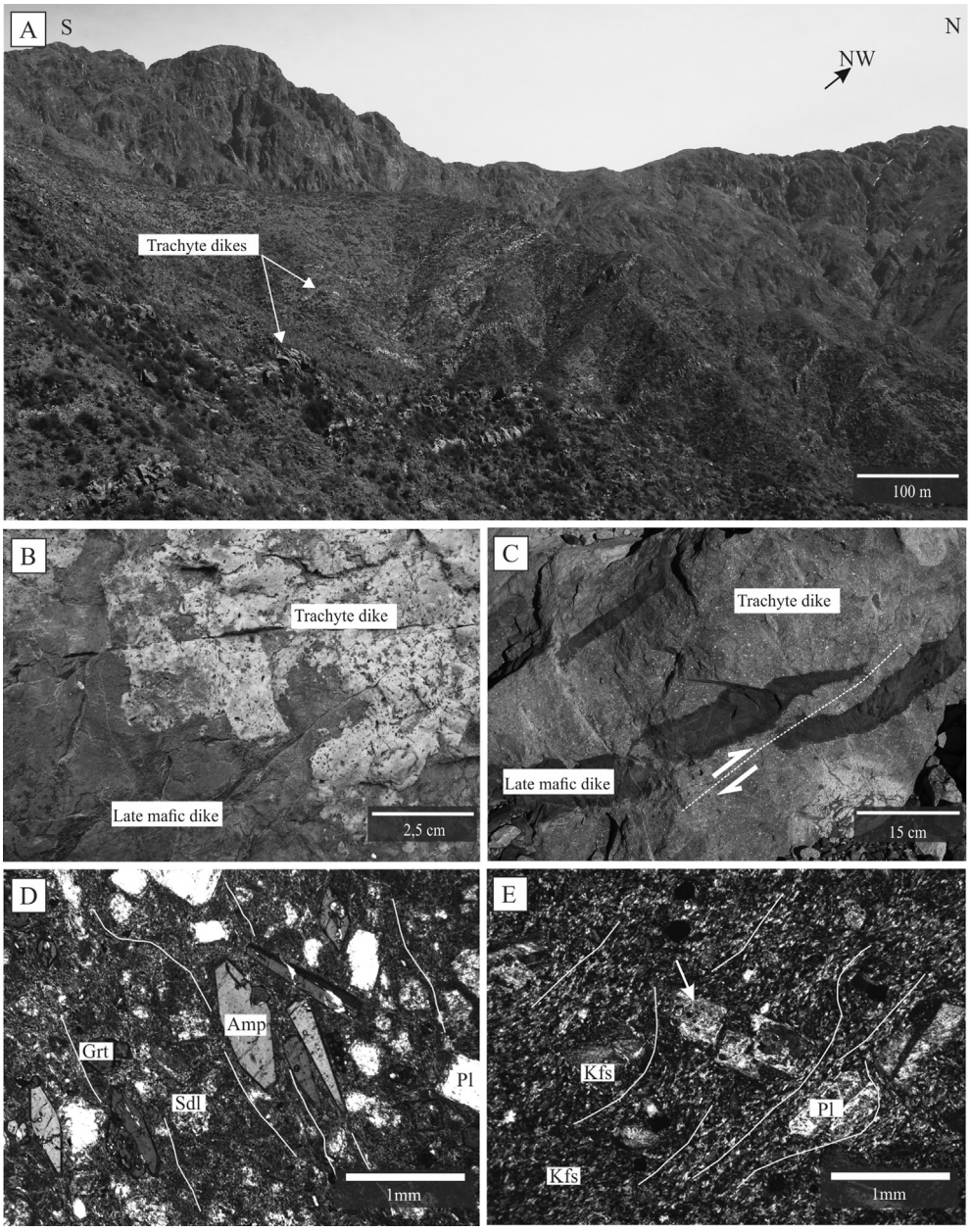

Fig. 10. Dikes system. A) Trachyte dikes with preferential NW–SE trend. B) Relations between mafic and trachytic dikes, the irregular contact reflect that both mafic and trachytic magmas still were liquids or slightly crystallized in the moment of intrusion. C) Synmagmatic shear in a trachyte, affecting a late mafic dike that intruded before total crystallizaton of the trachyte. D) and E) Photomicrographs showing internal flow in dikes of trachyte composition. E) A plagioclase crystal fractured in high temperature conditions is observed (white arrow), note the trachytic groundmass occupying the fractures within the crystal, denoting that it was deformed before crystallization of the groundmass. White lines indicate flow strike. Kfs: K-feldspar, Pl: Plagioclase, Sdl: Sodalite, Amp: Amphibole, Grt: Garnet.

are aligned and triangular interstitial spaces developed, comparable to the observations in the syenite of the LPC.

Structural studies indicate that magma transport is favored principally by subvertical extensional fractures NW–SE, through a mechanism where fracture propagation prevails (Clemens and Mawer, 1992; Petford, 1996). Applying these mechanisms to the LPC, numerous magma sheets would have quickly risen through vertical channels, originating an intense planar fabric that is very evident in the central syenite intrusive, were the plane flows follow the preferential strike NW–SE. The broad preservation of the magmatic fabric is consistent with a rapid cooling, where magma sheets coming into contact with one another crystallize rapidly and in tandem, a circumstance that prevents mixture of magmas and preserves magmatic foliation. This interpretation can be extrapolated to what D'Eramo et al. (2006, 2010) explained for the development of the internal fabric and emplacement of granitic plutons from Calmayo and El Hongo, Sierras Pampeanas de Córdoba, Argentina. Although there are differences in the type of the preserved structures and, fundamentally, in the magmatic systems in question, the petrographic evidences in the LPC are consistent with a rapid cooling. Among the evidences there may be mentioned: 1) seriate porphyritic and microporphyritic textures (Fig. 5E, Fig. 8A and E), 2) minerals with disequilibrium textures, the reaction borders in plagioclase could even denote rapid decompression and overcooling, 3) presence of very fine-textured mafic dikes (Fig. 5F), and 4) development of differentiates with pegmatite texture (Fig. 6E).

The absence of a significant contact metamorphism, which was only identified in a small aureole surrounding the malignite, in

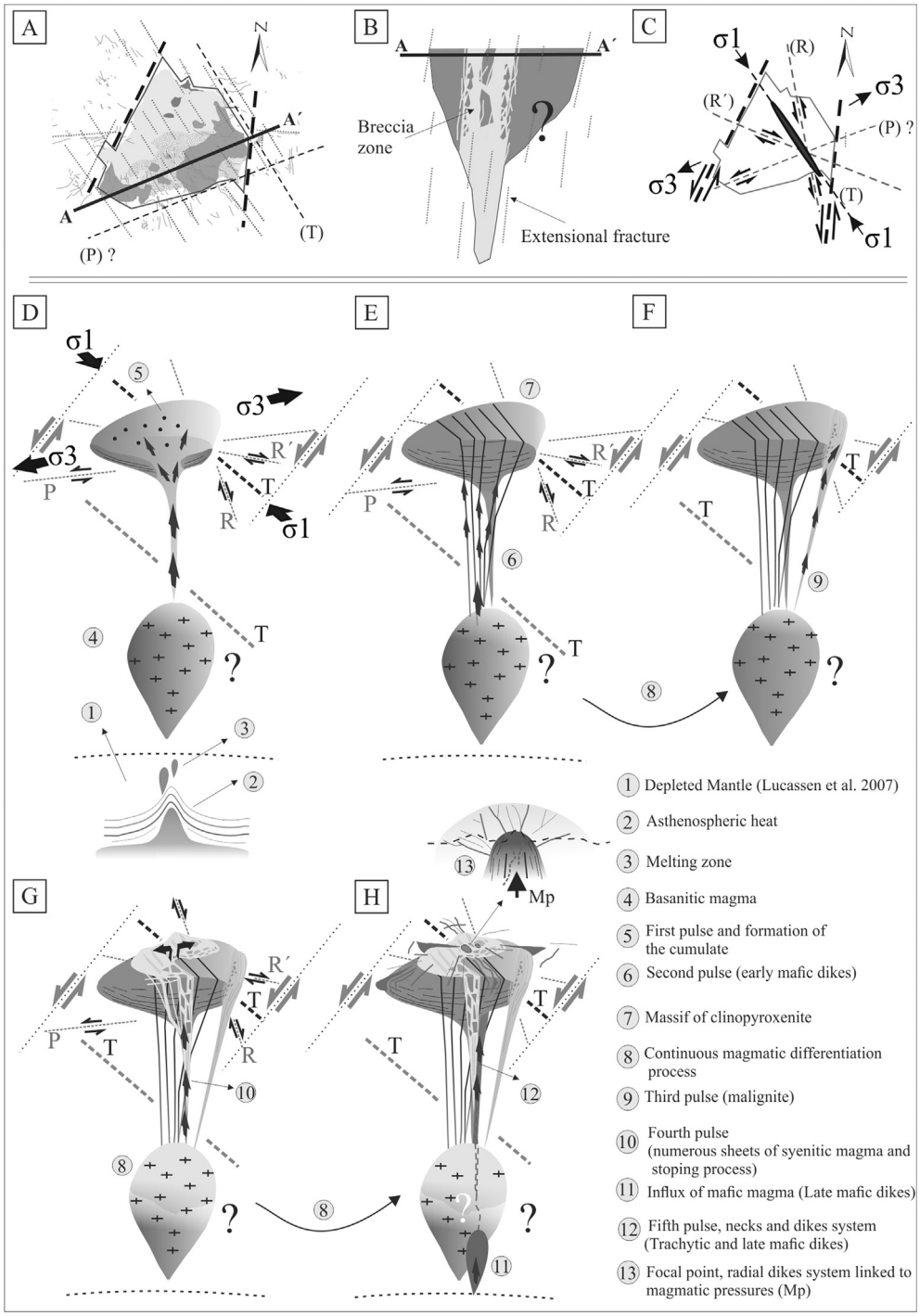

Fig. 11. Morphology of the complex and emplacement model. A) Scheme of the LPC showing how major fracture systems control morphology of the pluton. B) A–A′ cross-cut and hypothetical morphology of the body at depth. C) Scheme indicating the structures and their relationships with stress field. D), E), F), G) and H) 3D scheme of emplacement model, indicating the different magma pulses and related structures. D) Intrusion of a first pulse with composition close to basanite. E) Second pulse (Emd). F) Third pulse (malignite). G) Fourth pulse, ascent of numerous sheets of syenitic magma and intensive stoping processes allowing the development of the breccia zone and enabling an efficient transference material. H) Emplacement of porphyry necks and trachyte and Lmd; the magmatic pressures (MP) linked to the emplacement of the necks, favors the development of radial and annular fractures set, which allowed the magma intrusion.

addition to a shallow emplacement depth, could be attributed to short duration times of thermal disturbance due to an accelerated decay of the system, with consequent cooling of the magma.

Thus, the intrusion mechanism accounts for the compositional heterogeneity of the syenite intrusive. The syenite was formed by multiple pulses as parallel emplaced dikes, and these magma sheets show compositional, rheological and dynamic contrasts prior to crystallization and may have even experienced different cooling histories. The slight compositional variations may respond to active processes at depth, within the magma chambers. The developed flow planes currently represent non cohesive areas through which the rock fractures (Fig. 7F1).

The shape and type of contacts between magmatic units and the Villavicencio Formation (discordant, rectilinear and sharp contacts), numerous blocks and xenolitic clinopyroxenite forming magmatic breccias and annular and radial dikes can be explained only by brittle behavior, that is, stoping (e.g., Daly, 1903, 1933; Pinotti et al., 2002; Žák et al., 2006) and demonstrate the brittle host rock behavior which, weighted together with the petrographic features mentioned, allow establish that the magma in the LPC would have been emplaced at shallow crustal levels, in accordance with the crystallization temperature of Cc oxides as indicated by Zappettini et al. (2009).

5.2. Border of malignite facies: deformation by magma injection or shear phenomena?

The origin of foliation and deformation in the marginal zones of granitic plutons has been a topic of strenuous debate and some studies have suggested that magma injection into a crystallizing pluton causes its expansion (Sylvestre et al., 1978; Holder, 1979; Bateman, 1985; Courrioux, 1987; Ramsay, 1989), with consequent ductile deformation of already solidified margins. This case would occur in magmas with diapiric rise, but similar processes should take place if expansion occurs during growth of dike-fed plutons (Clemens and Mawer, 1992; Petford, 1996; Clemens et al., 1997). Nevertheless, solid state deformation of a crystallized border, attributed to magma expansion, is limited (Paterson, 1988; Paterson et al., 1991; Vernon and Paterson, 1993; Paterson and Vernon, 1995; Vernon, 2000). These processes should be less difficult if the border of the pluton contains small amounts of melt upon intrusion of the last magma pulses feeding it, thus favoring submagmatic flow (Paterson et al., 1989). While here it is not about granitic plutons, similar deformation phenomena are observed in the malignite facies borders. A certain evidence of submagmatic flow (primary nepheline and plagioclase crystals with wedges and fractures filled with interstitial material, Fig. 6I and J) and the effects of intracrystalline deformation (irregular extinction in K-feldspar, Fig. 6H) can be interpreted as the result of deformation localized on a border at an advanced stage of crystallization, with high crystalline fraction and small amounts of uncrystallized melt, represented by interstitial phases. Possibly the stress generated during forced magma injection would cause flattening of the border, similarly as indicated by Vernon et al. (2004) for the San José tonalite, Baja California, Mexico. The presence of an igneous autobreccia in the border facies is consistent with a magma injection interacting with a crystallized border, able to fracture and move, resulting in stoping phenomena. However, the presence of conjugate planes that have conditioned the orientation of tabular K-feldspar crystals might result from the high shear rates acting on the border of the intrusive and might respond to deformation phenomena synchronous with the intrusion of the LPC.

5.3. Garnet and amphibole, late interstitial phases?

Garnet (*melanite*) and amphibole are present occupying triangular interstitial spaces in both the central syenite and the maliginite facies (Fig. 6G, Fig. 8A and B). The texture relationships show that both minerals adapt to interstitial spaces and that the *melanite* crystals are replaced by the amphibole. Consequently, it can be considered that in this magmatic system these minerals may be the late crystallization phases, temporally equivalent to quartz and K-feldspar in granites. Andradite-type garnet rich in Ti, common in alkaline rocks (e.g., Dingwell and Brearley, 1985; Huggins et al., 1977; Keep and Russell, 1992; Vuorinen et al., 2005), also described in what Brod et al. (2003) called bebedourites, have been variably interpreted as primary or metasomatic (Flohr and Ross, 1990; Ulrych et al., 1994). These background data make it feasible to provisionally consider that the *melanite* of the LPC, at least the interstitial one, is of late crystallization.

5.4. Deep magma chamber

There are fairly clear petrographic evidences that the LPC does not represent evolutionary processes totally developed *in situ* in a magma chamber located at high crustal levels. Cross-cutting relationships among units, characteristics and shapes of contacts and the internal fabric of facies are the petrographic and structural indicators reflecting the interaction among the different magma pulses emplaced across crustal fractures at shallow levels and at different times. In this context, it is coherent to propose that the magma evolutionary process began at depth, in one or more reservoirs lodged in the lower crust, which originated the different pulses composing the igneous complex. This interpretation is additionally supported by the data obtained by Lucassen et al. (2007), who observed that the composition of Nd and Sr isotopes and the correlation of Pb isotopes indicate the mixture of melts from a depleted mantle, with small amounts of an isotopically different material. The signature of this contaminant, with non-radiogenic Nd and radiogenic Sr, represented by the isotopic relationships of two syenite samples, suggests that it would be crust material. Recently Zappettini et al. (2013) in the bases of trace element and isotopic data, indicate that all rock types of the LPC are derived from a common parental magma located in a reservoir at around 30 km depth.

The composition of the samples from the LPC denotes magmatic differentiation of the parental magma, and the clinopyroxenites have been considered to be cumulates of the most evolved rocks (Lucassen et al., 2007; Zappettini et al., 2013). According to Villar and Zappettini (2000), the initial magma with a composition close to that of the malignite would have produced the clinopyroxenite by sedimentation and the syenite and the system of dikes by fractionated crystallization. On the basis of the field relationships and the petrographic characteristics, it would be reasonable to think that the cumulate facies was segregated from an initial magma of approximately basanitic composition, which representative could currently be close to the malignite facies or alternatively to the Lmd. The isotopic results obtained by Zappettini et al. (2013) show a link between malignite and clinopyroxenite facies, whereas the Lmd are more radiogenic and deviate slightly from this isotopic field, which allows the authors to propose the malignite facies as the initial magma. However, our geochemical data (Pagano et al., in prep.) suggest that Lmd are more primitive than the malignite facies, and that there is a strong correspondence between the chemical composition of the clinopyroxene from the cumulate clinopyroxenite and those from the Lmd, and not between the clinopyroxene from the cumulate clinopyroxenite and those from the malignite facies. The isotopic composition of the Lmd could be influenced by chemical diffusivities during the interactions between both basanitic (Lmd) and trachytic magmas, mingling/mixing, as the field evidence suggests. In the context of magma mingling/mixing, experimental studies on magmatic systems indicate that chemical diffusivities vary widely for different elements and isotopes. Chemical diffusivity measurements on dacitic-rhyolitic melt systems indicate that isotopic equilibration proceeds faster than chemical equilibration, and that isotopic equilibration is faster for Sr than for Nd (Baker, 1989, 1990; Lesher, 1990). Isotopic investigation of the various components of composite and synplutonic dikes in some granites of the Sierra Nevada batholith (Barbarin, 1989) indicates that the initial mafic and felsic components of these dikes have different isotopic features and that the more hybrid components are isotopically equilibrated (Barbarin, 1989). The interactions between both basanitic (Lmd) and

trachytic magmas, documented in this paper, should be considered in isotopic interpretations, and lead further research to delve deeper into this field.

Villar et al. (2002) pointed out that the coarse pyroxenite facies is of a xenolithic nature and might be the base of a remobilized magma chamber. However, the intrusion relationships show not a remobilizing process but one of an *in situ* intrusion, where large blocks of the Cc are cross-cut by Emd.

5.5. Villavicencio fault system: western border of the shear zone?

The Villavicencio fault system, dividing the Precordillera into two structural domains with different deformation styles, would have allowed the partition of strain since, at least, the Middle Paleozoic. Models for compartmentalization of strain require pre-existence of a zone of weakness along which a simple shear component is accommodated (Jones and Tanner, 1995). Such weakness includes the Villavicencio fault, interpreted as representing a geologic anisotropy which is presently associated with the inferred suture zone between Chilenia and Cuyania terrains (Giambiagi et al., in press). Complementarily, the existence of mesoscale faults, with strike component and north-south shortening direction near the Villavicencio fault, first assigned to the Permian strike-slip event (Giambiagi et al., 2011) allows consider this complex deformation zone as the western branch of the shear zone. The eastern branch is considered here to be buried below of the modern sedimentary cover immediately to the east of the LPC. Within this context, the Villavicencio Formation, located between two shear zones, would have behaved as a rigid block favorable for fracturing, favoring development of the system of discontinuities that controlled magmatic melt circulation in the LPC.

5.6. Transtension in the retroarc at 18–19 Ma

The tectonic setting of emplacement of the LPC proposed by Zappettini et al. (2005) would be linked to a relaxation stage between two compression maximums occurred at 23 and 10 Ma; however, Zappettini et al. (2013) suggest back-arc extensional conditions during the latest Early Miocene (19 Ma), related to the geometry of the Pacific subducted plate beneath the South American plate. The structural analysis conducted in this research allows interpretation that the emplacement of the LPC is clearly favored by a possibly local transtensive regime, which would have developed during the early Miocene, ~19 Ma, in the retroarc of the Andes orogen, in what is now known as the Precordillera Mendocina morphostructural unit. At the same time, the compressive deformation was focused in the Principal Cordillera, 100 km westward of LPC with the development of the Aconcagua fold and thrust belt (Cegarra and Ramos, 1996). This compressive thin-skinned deformation belt (Ramos, 1985), would have started its development during the Early Miocene, 22–21 Ma (Charrier et al., 2005; Fock et al., 2006) in the Chilean region and would have extended eastwards since then. The onset of deformation in the western slope is marked by the change from low-K Abanico Formation tholeiites to calc-alkaline dacites of the Teniente Volcanic Complex (Kay et al., 2005, 2006), between 21 and 19 Ma (Charrier et al., 2002, 2005). This inversion occurred coevally with the development of the Farellones volcanic arc of Early to Middle Miocene age (Vergara et al., 1999). A 22.5 Ma U–Pb zircon Shrimp age of the base of the Farellones Formation along the Ramón-Damas Range anticline marks the beginning of the Farellones arc at this transect (Fock, 2005). At that time, the foreland was represented by an extensive peneplain, preserved at present in the different units that now form the Frontal Cordillera. Eastward migration of the deformation would have caused the uplift of the Frontal Cordillera at 10–9 Ma (Irigoyen et al., 1995) and the Precordillera (Walcek and Hoke, 2012). For this phase of compression and crustal shortening, Kay and Mpodozis (2002) argue that the reduced magmatic activity recorded in some regions over the interval 20–16 Ma could be explained by a mechanism of adjustment between two converging plates, due to changes in convergence parameters from an oblique to an orthogonal position. These changes at ~22 Ma would mark the beginning of the long period of Miocene compressive deformation and tectonic inversion along the flat-slab segment (Kay and Mpodozis, 2002). In dissidence to the model recently proposed by Zappettini et al. (2013) and considering this compressive geodynamic context, our data based on a detailed structural analysis, indicates the importance of a local strike-slip regime developed in the retroarc of the Andes orogen, during compression and shortening of the arc responsible, at the same latitude, for the development of the Aconcagua fold and thrust belt. On this basis we propose a model which explains the emplacement of the LPC in a transtensional environment.

6. Conclusions

The detailed structural and petrographic study of the LPC shows that, albeit displaying features that are frequent in other alkaline complexes worldwide, it has been emplaced under a tectonic control that has conditioned its magmatic fabric and even its inferred morphology.

The country rock fracturing system is genetically related to a brittle shear zone, and exhibits a *K*-type fractal fracture design represented by R, R′, P and T systems, which has controlled magma melt migration through the opening of the different branches, but particularly through extensional fractures (T).

The LPC would have been formed by juxtaposition of several magma pulses, derived from one or more deep chambers and emplaced at subvolcanic levels. The first emplaced pulse would have a composition close to that of basanite and its largest volume would have been fractionated, forming the clinopyroxenite cumulate; the second pulse is represented by the numerous Emd that cross-cut the Cc; the third phase is defined by the malignite, whereas the fourth pulse corresponds to the central syenite; and, finally, the last pulse has formed porphyry necks and the system of trachyte and Lmd.

The mechanism prevailing in the ascent of the magma is that of fracture propagation which, particularly for the LPC, corresponds to a northwest-southeast system genetically linked to a brittle shear zone; the different mechanisms that would have acted during the emplacement are summarized in: 1) opening of discontinuities synchronous to the magma circulation 2) stoping processes and 3) shear-related deformation (regional stress).

This system was active at 18–19 Ma (Early-Miocene) and was generated in a transtensive regime, locally developed in the retroarc of the Andes orogen, during full compression and shortening of the arc, responsible at the same latitudes, for development of the Aconcagua fold and thrust belt.

Acknowledgments

This study was made possible by the support of CONICET from Argentina through the grant PIP 11220090100857. DSP is also grateful to CONICET for the fellowships awarded to him; this paper is part of his Ph. D. The authors are grateful for the thorough review of the manuscript by L. Giambiagi and L. Pinotti, and for the editorial suggestions and corrections made by the Editor J. Kellogg. The authors are very grateful to A. Morosini, L. Giambiagi and J. Mescua for the insight in the field and to F. D'Eramo and L. Pinotti for their suggestions.

References

Allmendinger, R.W., Figueroa, D., Snyder, D., Beer, J., Mpodozis, C., Isacks, B.L., 1990. Foreland shortening and crustal balancing in the Andes at 30°S latitude. Tectonics 9, 789–809.

Arzamastsev, A.A., Glaznev, V.N., Raevsky, A.B., Arzamastseva, L.V., 2000. Morphology and internal structure of the Kola Alkaline intrusions, NE Fennoscandian Shield: 3D density modelling and geological implications. J. Asian Earth Sci. 18, 213–228.

Baker, D.R., 1989. Tracer versus trace element diffusion: diffusional decoupling of Sr concentration from Sr isotope composition. Geochim. Cosmochim. Acta 53 (11), 3015–3023.

Baker, D.R., 1990. Chemical interdiffusion of dacite and rhyolite: anhydrous measurements at 1 atm and 10 kbar, application of transition state theory, and diffusion in zoned magma chambers. Contribut. Mineral. Petrol. 104 (4), 407–423.

Barbarin, B., 1989. Importance des différents processus d'hybridation dans les plutons granitiques du batholite de la Sierra Nevada Californie. Schweiz. Mineral. Petrogr. Mittl. 69 (2), 303–315.

Barbosa, E.S.R., Brod, J.A., Junqueira-Brod, T.C., Dantas, E.L., Cordeiro, P.F.D.O., Gomide, C.S., 2012. Bebedourite from its type area (Salitre I complex): a key petrogenetic series in the Late-Cretaceous Alto Paranaíba kamafugite–carbonatite–phoscorite association, Central Brazil. Lithos 144, 56–72.

Bateman, R., 1985. Aureole deformation by flattening around a diaper during in situ ballooning: the Cannibal Creek granite. J. Geol. 93, 293–310.

Bell, K., Blenkinsop, J., 1987a. Nd and Sr isotopic compositions of East African carbonatites: implications for mantle heterogeneity. Geology 15, 99–102.

Bell, K., Blenkinsop, J., 1987b. Archean depleted mantle: evidence from Nd and Sr initial isotopic ratios of carbonatites. Geochim. Cosmochim. Acta 51 (2), 291–298.

Bergantz, G.W., 2000. On the dynamics of magma mixing by reintrusion: implications for pluton assembly processes. J. Struct. Geol. 22 (9), 1297–1309.

Bouchez, J.L., Delas, C., Gleizes, G., Nedelec, A., Cuney, M., 1992. Submagmatic microfractures in granites. Geology 20, 35–38.

Bouillin, J.P., Bouchez, J.L., Lespinasse, P., Pêcher, A., 1993. Granite emplacement in an extensional setting: an ASM of the magmatic structures of Monte capanne (Elba, Italy). Earth Planet. Sci. Lett. 118, 263–279.

Brod, J.A., Junqueira-Brod, T.C., Gaspar, J.C., Gibson, S.A., Thompson, R.N., 2003. Ti-rich and Ti-poor garnet from the Tapira Carbonatite complex, SE Brazil: fingerprinting fractional crystallisation and liquid immiscibility. In: 8th International Kimberlite Conference, Victoria. Extended Abstracts. FLA0339.

Brod, J.A., Gaspar, J.C., Diniz-Pinto, H.S., Junqueira-Brod, T.C., 2005. Spinel chemistry and petrogenetic processes in the tapira alkaline-carbonatite complex, Minas Gerais, Brazil. Braz. J. Geol. 35 (1), 23–32.

Buddington, A.F., 1959. Granite emplacement with special reference to North America. Geol. Soc. Am. Bull. 70, 671–747.

Cegarra, M.I., Ramos, V.A., 1996. La faja plegada y corrida del Aconcagua. Geología de la región del Aconcagua, provincias de San Juan y Mendoza. Subsecr. Minería la Nación, Dirección Nac. del Serv. Geológico, An. 24 (14), 387–422. Buenos Aires.

Charrier, R., Baeza, O., Elgueta, S., Flynn, J.J., Gans, P., Kay, S.M., Muñoz, N., Wyss, A.R., Zurita, E., 2002. Evidence for Cenozoic extensional basin development and tectonic inversion in the southern central Andes, Chile (33–36 S.L.). J. South Am. Earth Sci. 15 (1), 117–139.

Charrier, R., Bustamante, M., Comte, D., Elgueta, S., Flynn, J.J., Iturra, N., Muñoz, N., Pardo, M., Thiele, R., Wyss, A.R., 2005. The Abanico extensional basin: regional extension, chronology of tectonic inversion, and relation to shallow seismic activity and Andean uplift. Neues Jahrb. für Geol. Paläontologie Abh. 236 (1–2), 43–77.

Clarke, D.B., Henry, A.S., White, M.A., 1998. Exploding xenoliths and the absence of "elephants' graveyards" in granite batholiths. J. Struct. Geol. 20, 1325–1343.

Clemens, J.D., Mawer, C.K., 1992. Granitic magma transport by fracture propagation. Tectonophysics 204, 339–360.

Clemens, J.D., Petford, N., Mawer, C.K., 1997. Ascent mechanisms of granitic magmas: causes and consequences. In: Holness, M.B. (Ed.), Deformation-enhanced Fluid Transport in the Earth's Crust and Mantle. Chapman and Hall, London, pp. 144–171.

Courrioux, G., 1987. Oblique diapirism: the Criffel granodiorite/granite zoned pluton (southwest Scotland). J. Struct. Geol. 9, 313–330.

Cuerda, A., Cingolani, C., Bordonaro, O., 1993. Las secuencias sedimentarias eopaleozoicas. In: Ramos, V.A. (Ed.), Geología y Recursos Naturales de Mendoza, Congreso Geológico Argentino and Congreso de Exploración de Hidrocarburos, Relatorio, Mendoza, Asociación Geológica Argentina, vol. 1, pp. 21–30. Buenos Aires.

D'Eramo, F., Pinotti, L., Tubía Martínez, J.M., Vegas, N., Aranguren, A., Tejero, R., Gómez, D., 2006. Coalescence of lateral spreading magma ascending through dykes: a mechanism to form a granite canopy (El Hongo pluton, Sierras Pampeanas, Argentina). J. Geol. Soc. 163 (5), 881–892.

D'Eramo, F., Pinotti, L., Raniolo, A., Gómez, D., Coniglio, J., Demartis, M., ampanella, O., Tubía Martínez, J.M., Kostadinoff, J., 2010. Gravimetría del plutón Calmayo: implicancias en el ascenso y emplazamiento de magmas trondhemíticos. In: 10° Congreso de Mineralogía y Metalogenia, Río Cuarto, Actas, pp. 265–270.

Daly, R.A., 1903. The mechanics of igneous intrusion. Am. J. Sci. 165, 269–298.

Daly, R.A., 1933. Igneous Rocks and the Depths of the Earth. McGraw-Hill, New York.

Davis, J.S., Roeske, S.M., McClelland, W., Kay, S.M., 2000. Mafic and ultramafic crustal fragments of the southwestern Precordillera terrane and their bearing on tectonic models of the early Paleozoic in western Argentina. Geology 28, 171–174.

de Saint Blanquat, M., Tikoff, B., 1997. Development of magmatic to solidstate fabrics during syntectonic emplacement of the Mono Creek granite, Sierra Nevada Batholith, California. In: Bouchez, J.-L., Stephens, W.E., Hutton, D.E. (Eds.), Granite: From Melt Segregation to Emplacement Fabrics. Kluwer, Dordrecht, The Netherlands, pp. 231–252.

Dehls, J.D., Cruden, A.R., Vigneresse, J.L., 1998. Fracture control of late-Archean pluton emplacement in the Northern Slave Province, Canada. J. Struct. Geol. 20, 1145–1154.

Dingwell, D.B., Brearley, M., 1985. Mineral chemistry of igneous melanite garnets from analcite-bearing volcanic rocks, Alberta, Canada. Contribut. Mineral. Petrol. 90, 29–35.

Flohr, M.J.K., Ross, M., 1990. Alkaline igneous rocks of Magnet Cove, Arkansas: mineralogy and geochemistry of syenites. Lithos 26, 67–98.

Fock, A., 2005. Cronología y tectónica de la exhumación en el Neógeno de los Andes de Chile central entre los 33° y los 34°S. MS Thesis. Universidad de Chile, Chile.

Fock, A., Charrier, R., Marsaev, V., Farías, M., Alvarez, P., 2006. Evoluciónc enozoica de los Andes de Chile Central (33°–34°S). In: Proceedings of the 9°Congreso Geológico Chileno. Actas, vol. 2, pp. 205–208.

Folguera, A., Etcheverria, M., Pazos, P., Giambiagi, L., Cortés, J.M., Fauqué, L., Fusari, C., Rodriguez, M.F., 2001. Descripción de la Hoja Geológica Potrerillos (1: 100.000): Subsecretaría de Minería de la Nación. Dirección Nacional del Servicio Geológico, p. 262.

Furlong, K.P., Myers, J.D., 1985. Thermal-mechanical modeling of the role of thermal tresses and stoping in magma contamination. J. Volcanol. Geotherm. Res. 24, 179–191.

Gapais, D., Barbarin, B., 1986. Quartz fabric transition in a cooling syntectonic granite (Hermitage Massif, France). Tectonophysics 125, 357–370.

Giambiagi, L., Mescua, J., Bechis, F., Martínez, A., Folguera, A., 2011. Pre-Andean deformation of the Precordillera southern sector, southern Central Andes. Geosphere 7, 219–239.

Giambiagi, L., Mescua, J., Heredia, N., Farías, P., García Sansegundo, J., Fernández, C., Stier, S., Pérez, D., Bechis, F., Moreiras, S.M., Lossada, A., 2013. Reactivation of Paleozoic structures during Cenozoic deformation in the Cordón del Plata and Southern Precordillera ranges (Mendoza, Argentina). J. Iber. Geol. (in press).

Gonzalez Bonorino, G., 1975a. Sedimentología de la Formación Punta Negra y algunas consideraciones sobre la geología regional de la Precordillera de San-Juan y Mendoza. Rev. Asoc. Geológica Argent. 30 (3), 223–246.

Gonzalez Bonorino, G., 1975b. Acerca de la existencia de la Protoprecordillera de Cuyo. Actas 4° Congr. Geológico Argent. 1, 107.

Guillet, P., Bouchez, J.L., Vigneresse, J.L., 1985. Le compléxe granitique de Plouaret: mise en evidence structurale et gravimétrique de diapers emboités. Bull. la Societé Géologique Fr. 8, 503–513.

Harrington, H.J., 1941. Investigaciones geológicas en las sierras de Villavicencio y Mal Pais, Provincia de Mendoza. Dirección Minería Geol. Boletín N° 49, 54.

Holder, M.T., 1979. An emplacement mechanism for post-tectonic granites and its implications for their geochemical features. In: Atherton, M.P., Tarney, J. (Eds.), Origin of Granite Batholiths: Geochemical Evidence, Shiva, Orpington (Kent, UK), pp. 116–128.

Huggins, F.E., Virgo, D., Huckenholz, H.G., 1977. Titanium containing silicate garnets: II. the crystal chemistry of melanites and schorlomites. Am. Mineral. 62, 646–665.

Hutton, D.H.W., 1982. A tectonic model for the emplacement of the Main Donegal Granite, NW Ireland. J. Geol. Soc. 139 (5), 615–631.

Hutton, D.H.W., 1988. Granite emplacement mechanisms and tectonic controls: inferences from deformation studies. Trans. R. Soc. Edinb. Earth Sci. 79 (2–3), 245–255.

Hutton, D.H.W., Reavy, R.J., 1992. Strike-slip tectonics and granite emplacement. Tectonics 11, 960–967.

Hutton, D.H.W., Depster, T.J., Brown, P.E., Becker, S.D., 1990. A new mechanism of granite emplacement: intrusion in active extensional shear zones. Nature 343, 452–455.

Irigoyen, M.V., Brown, R.L., Ramos, V.A., 1995. Magnetic polarity stratigraphy and sequence of thrusting: 33°S latitude, Mendoza province, Central Andes of Argentina. In: COMTEC-ICL Andean Thrust Tectonics Symposium, Abstracts, pp. 16–17. San Juan.

Jones, R.R., Tanner, P.W.G., 1995. Strain partitioning in transpression zones. J. Struct. Geol. 17, 793–802.

Kay, S.M., Mpodozis, C., 2002. Magmatism as a probe to the Neogene shallowing of the Nazca plate beneath the modern Chilean flat-slab. J. South Am. Earth Sci. 15, 39–57.

Kay, S.M., Godoy, E., Kurtz, A., 2005. Episodic arc migration, crustal thickening, subduction erosion, and magmatism in the south-central Andes. Geol. Soc. Am. Bull. 117, 67–88.

Kay, S.M., Burns, M., Copeland, P., Mancilla, O., 2006. Upper Cretaceous to Holocene magmatism and evidence for transient Miocene shallowing of the Andean subduction zone under the northern Neuquén Basin. In: Kay, S.M., Ramos, V.A. (Eds.), Evolution of an Andean Margin: A Tectonic and Magmatic View from the Andes to the Neuquén Basin (35°–39°S Lat): Boulder, Colorado, Geological Society of America Special Paper, vol. 407, pp. 19–60.

Keep, M., Russell, J.K., 1992. Mesozoic alkaline rocks of the Averill plutonic complex. Can. J. Earth Sci. 29, 2508–2520.

Kogarko, L.N., Kononova, V.A., Orlova, M.P., Woolley, A.R., 1995. Alkaline Rocks and Carbonatites of the World: Part 2. Former USSR. Chapman and Hall, London, p. 225.

Larsen, L.M., Rex, D.C., 1992. A review of the 2500 Ma span of alkaline–ultramafic, potassic and carbonatitic magmatism in West Greenland. Lithos 28, 367–402.

Le Bas, M.J., 1977. Carbonatite–Nephelinite Volcanism. An African Case History. Wiley, London, p. 347.

Le Maitre, R.W., 2002. Igneous Rocks: a Classification and Glossary of Terms: Recommendations of the International Union of Geological Sciences Subcommission on the Systematics of Igneous Rocks. Cambridge University Press, Cambridge.

Lesher, C.E., 1990. Decoupling of chemical and isotopic exchange during magma mixing. Nature 344, 235–237.

Lucassen, F., Franz, G., Romer, R.L., Schultz, F., Dulski, P., Wemmer, K., 2007. Pre-Cenozoic intra-plate magmatism along the Central Andes (17–34°S): composition of the mantle at an active margin. Lithos 99, 312–338.

Marsh, B.D., 1982. On the mechanics of igneous diapirism, stoping, and zone melting. Am. J. Sci. 282, 808–855.

McCoss, A.M., 1986. Simple constructions for deformation in transpression/transtension zones. J. Struct. Geol. 8 (6), 715–718.

Méndez, V., Zanettini, J.C., Zappettini, E.O., 1995. Geología y Metalogénesis del Orógeno Andino Central, República Argentina. Dirección Nac. Serv. Geológico, An. 23 (Buenos Aires, Argentina).

Mezzetti, A.M., 1968. Informe final zona "Puesto La Peña", Área de reserva N° 5, Provincia de Mendoza, República Argentina (inédito). Dirección General de Fábricaciones Militares, Buenos Aires, Argentina, p. 6, 4 anexos.

Morbidelli, L., Gomes, C.B., Beccaluva, L., Brotzu, P., Conte, A.M., Ruberti, E., Traversa, G., 1995. Mineralogical, petrological and geochemical aspects of alkaline and alkaline–carbonatite association from Brazil. Earth Sci. 39, 135–168.

Morosini, A., Ortiz Suárez, A., Carugno Durán, A., 2012. Estructura del distrito volcánico La Carolina, provincia de San Luis. In: Actas de la XV Reunión de Tectónica. San Juan, pp. 97–98.

Mpodozis, C., Ramos, V.A., 1989. The Andes of Chile and Argentina. In: Ericksen, G.E., Cañas, M.T., Reinemud, J.A. (Eds.), Geology of the Andes and its Relation to Hydrocarbon and Mineral Resources, Circum-Pacific Council for Energy and Mineral Resources Earth Science Series, vol. 11, pp. 59–90.

Nielsen, T.F., 1980. The petrology of a melilitolite, melteigite, carbonatite and syenite ring dyke system, in the Gardiner complex, East Greenland. Lithos 13, 181–197.

Paterson, S.R., 1988. Cannibal Creek granite: post-tectonic "ballooning" pluton or pre-tectonic piercement diapir? J. Geol. 96, 730–736.

Paterson, S.R., Vernon, R.H., 1995. Bursting the bubble of ballooning plutons: a return to nested diapirs emplaced by multiple processes. Bull. Geol. Soc. Am. 107, 1356–1380.

Paterson, S.R., Vernon, R.H., Tobisch, O.T., 1989. A review of criteria for the identification of magmatic and tectonic foliations in granitoids. J. Struct. Geol. 11, 349–363.

Paterson, S.R., Brudos, T., Fowler, K., Carlson, C., Bishop, K., Vernon, R.H., 1991. Papoose Flat pluton: forceful expansion or post-emplacement deformation? Geology 19, 324–327.

Paterson, S.R., Fowler, T.K., Miller, R.B., 1996. Pluton emplacement in arcs: a crustal exchange process. Trans. R. Soc. Edinb. Earth Sci. 87, 115–123.

Paterson, S.R., Fowler Jr., K., Schmidt, K.L., Yoshinobu, A.S., Semele Yuan, E., Miller, R., 1998. Interpreting magmatic fabric patterns in plutons. Lithos 44 (1–2), 53–82.

Peacock, D.C.P., Sanderson, D.J., 1995. Pull-apart, shear fractures and pressure solution. Tectonophysics 241, 1–13.

Petford, N., 1996. Dykes or diapirs? Trans. R. Soc. Edinb. Earth Sci. 87 (1–2), 105–114.

Petford, N., Cruden, A.R., McCaffrey, K.J.W., Vigneresse, J.L., 2000. Dynamics of granitic magma formation, transport and emplacement in the Earth's crust. Nature 408, 669–673.

Pignotta, G.S., Paterson, S.R., 2007. Voluminous stoping in the Mitchell Peak granodiorite, Sierra Nevada batholith, California, USA. Can. Mineral. 45 (1), 87–106.

Pinotti, L.P., Coniglio, J.E., Esparza, A.M., D'Eramo, F.J., Llambıas, E.J., 2002. Nearly circular plutons emplaced by stoping at shallow crustal levels, Cerro Aspero batholith, Sierras Pampeanas de Córdoba, Argentina. J. South Am. Earth Sci. 15 (2), 251–265.

Pinotti, L.P., D'Eramo, F.J., Demartis, M., Coniglio, J.E., Tubía Martínez, J.M., 2010. Estructuras magmáticas en granitos. Rev. la Asoc. Geológica Argent. 67 (4), 562–572.

Ramos, V.A., 1985. El Mesozoico de la Alta Cordillera de Mendoza: facies y desarrollo estratigráfico. Argentina 4 Cong. Geol. Chileno, Antofagasta. Actas 1, 492–513.

Ramos, V.A., 1988. The tectonics of the Central Andes: 30° to 33° S latitude. In: Clark, S., Burchfiel, D. (Eds.), Processes in Continental Lithospheric Deformation, Geological Society of America Special Paper, vol. 218, pp. 31–54.

Ramos, V.A., Jordan, T., Allmendinger, R., Mpodozis, C., Kay, S.M., Cortés, J.M., Palma, M.A., 1986. Paleozoic terranes of the Central Argentine–Chilean Andes. Tectonics 5, 855–880.

Ramsay, J.G., 1989. Emplacement kinematics of a granite diapir: the Chindamora batholith, Zimbabwe. J. Struct. Geol. 11, 191–210.

Ribeiro, C.C., Brod, J.A., Junqueira-Brod, T.C., Gaspar, J.C., Petrinovic, I.A., 2005. Mineralogical and field aspects of magma fragmentation deposits in a carbonate–phosphate magma chamber: evidence from the Catalão I complex, Brazil. J. South Am. Earth Sci. 18, 355–369.

Sanderson, D.J., Marchini, W.R.D., 1984. Transpression. J. Struct. Geol. 6 (5), 449–458.

Sibson, R.H., 1990. Conditions for Fault-valve Behaviour. In: Geological Society, London, Special Publications, vol. 54(1), pp. 15–28.

Sibson, R.H., 1996. Structural permeability of fluid-driven fault-fracture meshes. J. Struct. Geol. 18 (8), 1031–1042.

Sibson, R.H., 2000. Fluid involvement in normal faulting. J. Geodyn. 29 (3), 469–499.

Sylvester, A.G., Oertel, G., Nelson, C.A., Christie, J.M., 1978. Papoose flat pluton: a granite blister in the Inyo Mountains, eastern California. Bull. Geol. Soc. Am. 89, 1205–1219.

Tobish, O.T., Paterson, S.R., 1990. The Yarra granite: an intradeformational pluton associated with ductile thrusting, Lachlan Fold Belt, southeastern Australia. Geol. Soc. Am. Bull. 102, 693–703.

Traversa, G., Gomes, C.B., Brotzu, P., Buraglini, N., Morbidelli, L., Principato, M.S., Ruberti, E., 2001. Petrography and mineral chemistry of carbonatites and mica-rich rocks from the Araxá complex (Alto Paranaíba Province, Brazil). An. Acad. Bras. Ciências 73 (1), 71–98.

Ulrych, J., Povondra, P., Pivec, E., Rutsek, J., Sitek, J., 1994. Compositional evolution of metasomatic garnet inmelilitic rocks of the Osecna complex, Bohemia. Can. Mineral. 32, 637–647.

Valadares, V., González-Clavijo, E.J., 2004. Nuevos datos sobre la geología del complejo alcalino de Monchique (SW de Portugal). Geogaceta 36, 39–42.

Vegas, N., Tubía, J.M., Esteban, J.J., Cuevas, J., 2007. Distribución de la deformación en granitoides sincinemáticos intruidos en condiciones transpresivas (Sanabria, Zona Centro-Ibérica, Macizo Ibérico). Geogaceta 43, 23–26.

Vergara, M., Morata, D., Villarroel, R., Nyström, J., Aguirre, L., 1999. Ar/Ar ages, very low-grade metamorphism and geochemistry of the volcanic rocks from "Cerro El Abanico", Santiago Andean Cordillera (33°30′S-70° 30′-70° 25′W). In: Proceedings of the IV International Symposium on Andean Geodynamics, Göttingen, Germany, pp. 785–788.

Vergés, J., Ramos, V.A., Meigs, A., Cristallini, E., Bettini, F.H., Cortés, J.M., 2007. Crustal wedging triggering recent deformation in the Andean thrust front between 31°S and 33°S: Sierras Pampeanas-Precordillera interaction. J. Geophys. Res. v. 112.

Vernon, R.H., 2000. Review of microstructural evidence of magmatic and solid-state flow. Electron. Geosci. 5 (2), 1–23.

Vernon, R.H., Paterson, S.R., 1993. The Ardara pluton, Ireland: deflating an expanded intrusion. Lithos 31, 17–32.

Vernon, R.H., Johnson, S.E., Melis, E.A., 2004. Emplacement-related microstructures in the margin of a deformed pluton: the San José tonalite, Baja California, México. J. Struct. Geol. 26, 1867–1884.

Villar, L.M., Zappettini, E.O., 2000. El Complejo alcalino Paleógeno de Puesto La Peña. In: Simposio Internacional Magmatismo Andino. 9° Congreso Geológico Chileno. Actas, vol. 2, pp. 697–701.

Villar, L.M., Zappettini, E.O., Hernández, L., 2002. Mineralogía del Complejo alcalino Puesto La Peña, Provincia de Mendoza Argentina. Mineral. Metalog., 453–460.

von Gosen, W., 1992. Structural evolution of the Argentine Precordillera: Río San Juan section. J. Struct. Geol. 14, 643–667.

von Gosen, W., 1995. Polyphase structural evolution of the southwestern Argentine Precordillera. J. South Am. Earth Sci. 8, 377–404.

Vuorinen, J.H., Halenius, U., Whitehouse, M.J., Mansfeld, J., Skelton, A.D.L., 2005. Compositional variations (major and trace elements) of clinopyroxene and Ti-andradite from pyroxenite, ijolite and nepheline syenite, Alno Island, Sweden. Lithos 81, 55–77.

Walcek, A.A., Hoke, G.D., 2012. Surface uplift and erosion of the southernmost Argentine Precordillera. Geomorphology 153, 156–168.

Yoshinobu, A.S., Fowler Jr., T.K., Paterson, S.R., Llambias, E., Tickyj, H., Sato, A.M., 2003. A view from the roof; magmatic stoping in the shallow crust, Chita Pluton, Argentina. J. Struct. Geol. 25, 1037–1048.

Žák, J., Holub, F.V., Kachlík, V., 2006. Magmatic stoping as an important emplacement mechanism of Variscan plutons: evidence from roof pendants in the Central Bohemian Plutonic Complex (Bohemian Massif). Int. J. Earth Sci. 95 (5), 771–789.

Zappettini, E.O., Basei, M.A., Villar, L., Teixeira, W., 2005. Edad de la facies malignita del Complejo Alcalino Puesto La Peña, Mendoza, Argentina. In: Cabaleri, N., Cingolani, C.A., Linares, E., López de Luchi, M.G., Ostera, H.A., Panarello, H.O. (Eds.), Actas del XVI Congreso Geológico Argentino, Artículo N°, vol. 537, p. 6.

Zappettini, E.O., Brodtkorb, M.K., Bernhardt, H.J., Villar, L., 2008. Sobre los espinelos del complejo alcalino Puesto La Peña, provincia de Mendoza. In: Actas del XVII Congreso Geológico Argentino. Jujuy, p. 695.

Zappettini, E.O., Brodtkorb, M.K., Bernhardt, H.J., Villar, L.M., 2009. Los espinelos del complejo alcalino Puesto La Peña, provincia de Mendoza. Rev. la Asoc. Geológica Argent. 64 (3), 544–549.

Zappettini, E.O., Villar, L.M., Hernández, L.B., Santos, J.O., 2013. Geochemical and Isotopic Constraints on the Petrogenesis of the Puesto La Peña Undersaturated Potassic Complex, Mendoza Province, Argentina, vols. 162–163. Geodynamic Implications, Lithos, pp. 301–316.